



HAL
open science

Creep Prediction of an Undisturbed Sensitive Clay

Gilberto Alexandre, Ian Martins, Paulo Santa Maria

► **To cite this version:**

Gilberto Alexandre, Ian Martins, Paulo Santa Maria. Creep Prediction of an Undisturbed Sensitive Clay. 2013. hal-00880388

HAL Id: hal-00880388

<https://hal.science/hal-00880388>

Submitted on 6 Nov 2013

HAL is a multi-disciplinary open access archive for the deposit and dissemination of scientific research documents, whether they are published or not. The documents may come from teaching and research institutions in France or abroad, or from public or private research centers.

L'archive ouverte pluridisciplinaire **HAL**, est destinée au dépôt et à la diffusion de documents scientifiques de niveau recherche, publiés ou non, émanant des établissements d'enseignement et de recherche français ou étrangers, des laboratoires publics ou privés.

Creep Prediction of an Undisturbed Sensitive Clay

Alexandre, G. F., D.Sc.

Martins, I.S.M., D.Sc., Associate Professor, COPPE/UFRJ, Rio de Janeiro, Brazil.

Santa Maria, P.E.L., Ph.D., Senior Specialist Engineer, Subsea7, Rio de Janeiro, Brazil

Abstract

This paper presents numerical predictions for the behavior of the sensitive marine Haney Clay subject to undrained creep and constant load tests. The predictions were carried-out based on the framework model proposed by Martins (1992) and in accordance with concepts developed by Terzaghi (1941), Taylor (1942, 1948), Bea (1960), Lo (1969a, 1969b), Bjerrum (1973), Finn and Snead (1973), Vaid and Campanella (1977) and others. The complete differential equations as well as simple numerical procedures used to predict the undrained creep and constant load tests are presented. In addition, analytical solutions are presented for the simplified differential equations of both undrained creep and constant load tests. It is shown that satisfactory predictions were achieved both qualitatively and quantitatively for most of the 11 undrained creep and 9 constant load tests.

Keywords

Undrained creep. Constitutive equations. Soil behavior. Strain rate effects. Time effects. Viscosity. Adsorbed water layer.

Introduction

Clays present time-dependent behavior. Experimental evidence of this behavior based on consolidation and shear strength characteristics have been presented by Buisman (1936), Taylor (1942, 1948), Casagrande & Wilson (1950), Murayama & Shibata (1958), Bishop and Henkel (1962), Mitchell et al. (1968), Crawford (1964), Bishop and Lovenbury (1969), Bjerrum (1973), Finn and Snead (1973), Lacerda (1976), Vaid and Campanella (1977), Tavenas et al (1978), Mesri et al (1981), Leroueil et al (1985), Martins (1992) and others.

The study presented herein deals with the behavior of clays subjected to shearing under undrained loadings and is applied to the tests carried-out by Vaid and Campanella (1977) on the Haney Clay. In more specific terms, this study aims to answer the following questions regarding the undrained creep behavior of a saturated clay:

- Will failure occur to a clay specimen subjected to a given stress state?
- If the specimen fails, how long will it take to fail? And;
- If not, what will be the final state of strain of the specimen and how long will it take for the specimen to reach it?

To answer these questions, the model developed by Martins (1992) for saturated clayey soils, as modified by Alexandre (2006), was used.

Previous Studies and Approaches

It seems that Casagrande and Wilson (1951) were among the first investigators to study creep and the effects of rate of loading on the shear characteristics of soils. They showed that soil specimens subjected to undrained creep loadings failed with deviatoric stresses in the range of 40% to 80% of the maximum deviatoric stresses of conventional tests.

Bishop and Lovenbury (1969) carried-out long term drained creep tests on London Clay as well as on Pancone Clay that lasted for about 3.5 years. They observed the lack of secondary or steady-state creep and demonstrated the limitation of the power law or logarithmic functions in representing strain vs time curves.

Finn and Snead (1973) carried out undrained creep tests on the Haney Clay. The specimens were left with closed drainage prior to the shearing phase for 8 hours when most of the pore-pressure dependent on the secondary consolidation developed. The investigators observed the lack of secondary (steady-state) creep. They attributed the start of failure to the minimum strain rate of creep tests and to an upper yielding strength. Also, according to them, specimens subjected to deviatoric stresses below the upper yielding strength would not fail and specimens subjected to deviatoric stresses greater than the upper yielding strength would fail. They also proposed an equation for the upper yielding strength, reproduced below:

$$\sigma_d = \sigma_{uy} + K \cdot \dot{\epsilon}^{1/n} \quad (1)$$

Where:

σ_d is the maximum deviatoric stress in a constant strain rate test or the deviatoric stress in a creep test;

σ_{uy} is the upper yielding strength;

$\dot{\epsilon}$ is the strain rate in a constant strain rate test or the transient minimum strain rate in a creep test; and

K and n are constants;

For the Haney Clay the authors found that $n = 3$, a value which was confirmed by Sherif (1965) for the clays of Seattle.

According to Finn and Snead (1973), the idea of an upper yielding strength is also postulated by Murayama and Shibata (1961) and by Vialov and Skibitsky (1957).

Bjerrum (1973), accepting that the shear strength can be represented by the parameters proposed by Hvorslev, explains a mechanism for creep mentioned in Schmertmann and Hall (1961) and proposed by Bea (1960).

According to Bjerrum, if the applied stress in a creep test is not greater than the maximum friction resistance available, the cohesion, which is fully mobilized for very small strains at the beginning of the test, would eventually be entirely transferred to friction with creep deformations coming to an end. On the other hand, if the applied stress is greater than the available friction, the transference of cohesion to friction will continue until all the available friction is mobilized. However, because the applied stress is greater than the available friction, the difference between the stress applied and friction will be carried by the cohesion. As the cohesion is assumed to be strain rate dependent, the strain rate will decrease until all the available friction is mobilized and remain constant thereafter.

Having these concepts in mind, the creep process involves the transference of “effective cohesion” to “effective friction”.

Vaid and Campanella (1977) carried out several strength tests to simulate various deformation rate histories. Tests such as creep (constant stress), constant load, constant rate of loading, constant rate of strain and step creep were carried out on the Haney Clay. The intent was to test the hypotheses that the shear stress, q , is a function of the strain, ϵ , as well as the strain rate, $\dot{\epsilon}$. That is $q = q(\epsilon, \dot{\epsilon})$.

The authors were able to show that the relationship between these variables holds throughout the entire creep process for the Haney Clay, even when the strain rate reaches a minimum and starts to increase again.

They also showed that the minimum strain rate for the Creep Test corresponds to a strain of about 2.5%, which is close to the strains at maximum deviatoric stress of the Constant Rate of Strain Test.

With regards to models for explaining creep behavior, one of the main models is the Rate Process Theory. This theory was developed in the area of Physical Chemistry and was originally intended for assessing the speed at which chemical reactions occur. Various investigators such as Murayama and Shibata (1958), Mitchell et al (1968) and Anderson and Douglas (1970) applied the Rate Process Theory to soil mechanics with success. It is recommended that works by Glasstone et al. (1940) as well as Mitchell et al (1968) be referred to for the fundamentals of this theory.

Other models for assessing creep include visco-elastic, visco-plastic or visco-elasto-plastic models combined with or not with the Rate Process Theory or the $c_{\alpha\epsilon}$ concept. A few of the models in this category were described by Murayama and Shibata (1958, 1961, 1964), Mesri et al (1981), Adachi and Okano (1974), Sekigushi (1984) and Kutter and Sathialingam (1992). As it will be seen in the following section the model developed by Martins' (1992) falls within this category.

Basic concepts of Martins' Model (1992)

According to Terzaghi (1941), the contact between clay particles can be separated into “solid bonds” and “film bonds”. In his view, both contacts are able to transmit effective stresses and would result from the adsorbed water layers that surround the clay particles. The “solid bonds” would result from the contact between the adsorbed water layers in the immediate vicinity of the clay particle, which, according to Terzaghi, would be in the solid state. The “film bonds” would result from the contact between adsorbed water layers which would not be in the solid state but which would possess a higher viscosity than the viscosity of the free water (by free water it refers to the water that flows out of the voids between soil particles during seepage or consolidation).

Having this picture in mind, Martins assumes as a hypothesis that the shear strength of a saturated normally consolidated clay has two components; the frictional resistance and the viscous resistance. The frictional resistance would develop between Terzaghi's “solid bonds” and it would be a function of the shear strain. The viscous resistance would develop between Terzaghi's “film bonds” and it would be a function of the strain rate. The equation for shear strength would then be:

$$\tau = \sigma' \cdot tg\phi'_{mob} + \eta(e) \cdot \dot{\epsilon} \quad (2)$$

Where:

σ' is the normal effective stress (taken as the difference between the normal total stress, σ , and pore-pressure, u);

ϕ'_{mob} is the mobilized effective angle of internal friction;

$\eta(e)$ is the coefficient of viscosity of the adsorbed water layer surrounding the clay particles (a function of void ratio for a normally consolidated clay); and

$\dot{\epsilon}$ is the strain rate.

The model assumed that pore-pressure that develops in a shear test would be a function of the shear strains as shown by Lo (1969a, 1969b). In addition, it is assumed in the model that normalization is valid. In other words, both the frictional and viscous resistances are proportional to consolidation pressure, σ'_c , and are a function of Over Consolidation Ratio (OCR). Equation (2) is similar to the

equation proposed by Taylor (1948).

Mechanism of Creep – Modified Martins’ Model

Alexandre (2006) modified Martins’ model by replacing Equation (2) by the following:

$$\sigma_d = \sigma_{df}(\varepsilon) + K(e) \cdot \dot{\varepsilon}^n \quad (3)$$

Where:

σ_d is the deviatoric stress of a creep test;

σ_{df} is the deviatoric friction resistance (considered a function of the shear strain for normally consolidated soils);

K and n are constants (K is also a function of the consolidation pressures, σ'_c).

Equation (3) can be seen as a generalization of the equation proposed by Finn and Snead (1973) and is consistent with the hypothesis raised by Vaid and Campanella (1977), where the shear stress, q , is a function of strain, ε , and the strain rate, $\dot{\varepsilon}$.

The mechanics of creep can be understood with the aid of Equation (3) and the Figure below, where two creep tests are represented together with what is called in accordance to Martins’ model, the “basic” deviatoric curve for a normally consolidated clay.

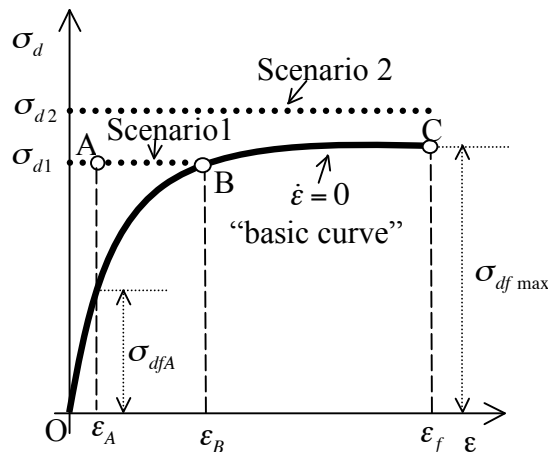


Figure 1 – Deviatoric stress x strain curves for two creep tests

The “basic” deviatoric curve is the component of the strength which is independent of rate or time effects. This curve is the one that would be obtained in a test where the strain rate is zero, provided such a test could be carried out. In addition, a Creep Test is a strength test where the deviatoric stress is held constant throughout its duration.

Scenario 1 will be analyzed first. As can be seen in Figure 1, the maximum frictional deviatoric stress is $\sigma_{df \max}$, which occurs for a given shear strain, ε_f . At the beginning of Test 1, at $t = 0$, the deviatoric stress, $\sigma_{d1} < \sigma_{df \max}$ is applied instantaneously. Considering Equation (3) and Figure 1, the vertical distance between the curve of Test 1 and the “basic” curve is therefore the viscous resistance. Therefore, at this point, the viscous resistance is identical to the applied deviatoric stress, σ_{d1} . At this point $\dot{\varepsilon}$ assumes the value $\dot{\varepsilon} = (\sigma_d / K)^{1/n}$. After some time, at Point A, the frictional resistance will be σ_{dfA} , relative to shear strain ε_A . At Point A, because of Equation (3), the viscous

resistance will be smaller than before, assuming the value $\dot{\epsilon} = \left[(\sigma_{d1} - \sigma_{dfA}) / K \right]^{1/n}$. As the process continues, the frictional resistance is mobilized and the viscous resistance is demobilized, with continuously decreasing strain rate, to balance Equation (3). Because Creep Test 1 has an applied deviatoric stress $\sigma_{df1} < \sigma_{df \max}$, the transference of viscous resistance to frictional resistance will continue until the frictional resistance equals the applied deviatoric stress, at Point B. At this point, the viscous resistance and the strain rate are both equal to zero and the shear strain is ϵ_B .

The same process occurs in Scenario 2, but, because the applied deviatoric stress is now greater than the maximum frictional resistance, there will not be not enough frictional resistance to be mobilized. At Point C, where the frictional resistance is maximum, the viscous resistance will be minimum and equal to $\sigma_{d2} - \sigma_{df \max}$ and the strain rate will be $\dot{\epsilon} = \left[(\sigma_{d2} - \sigma_{df \max}) / K \right]^{1/n}$. From this point on, the soil will continue to creep at constant strain rate indefinitely.

Having in mind the two Creep Tests described above, creep, in the light of the model developed by Martins, would be the process of transference of viscous resistance to frictional resistance with time, and failure in a creep test would be achieved when $\dot{\epsilon} > 0$ and when $\ddot{\epsilon} \geq 0$. Failure, in other words, would be achieved when all the available frictional resistance is mobilized and the soil element still continuous to deform at a constant strain rate or with a strain rate that increases with time.

The transference of viscous resistance to frictional resistance during creep as idealized in Martins' Model is in general agreement with the creep failure criteria proposed by Bea (1960).

The creep process explained here is able to explain the so-called "primary" stage of creep, where the strain rate decreases with time, and "secondary" stage of creep, where the strain rate remains constant with time, but is unable to explain the "tertiary" creep, where the strain rate increase with time. However, a conjecture for the increase in time of the strain rate observed during the "tertiary" stage of creep is presented below, based on Figure 2.

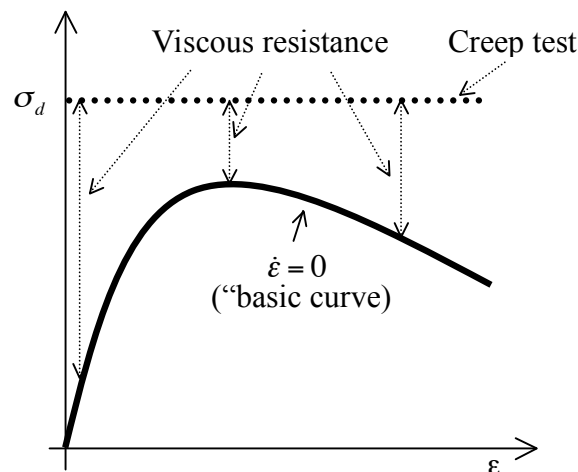


Figure 2 – Conjecture for explaining the "tertiary" creep

According to Figure 9, the frictional resistance no longer reaches a plateau in strength but instead passes through a peak. In other words, the frictional resistance, which is initially zero for shear strain equal to zero, increases with time, reaches a maximum value and then starts to decrease again. This behavior can be observed in over-consolidated clays, sensitive soils or whenever the pore-pressure continues to increase with time after the soil have reached the maximum shear strength. In addition to these cases, even normally consolidated clays can experience a peak, as long

as large deformations occur. In this case the maximum shear strength observed decreases until the residual strength is reached.

Referring to Figure 2 and also to Equation (3), the difference between the applied deviatoric stress and the frictional resistance is the viscous resistance. As the frictional resistance increases with the development of shear strains, reaches a peak and starts to decrease, the viscous resistance will have the opposite behavior. That is, the viscous resistance will decrease, pass through a minimum and then starts to increase again. Because the viscous resistance is proportional to the strain rate, the strain rate, as well, will decrease with time, reach a minimum (at the peak strain) and then start to increase again. This possible explanation for the tertiary creep was studied by Alexandre (2006) for the tests carried out by Vaid and Campanella (1977) on the sensitive Haney clay and will be explained in details in this paper.

Another conjecture for explaining the tertiary creep is a reduction in the coefficient of viscosity with the development of shear strains. If the coefficient of viscosity is shear strain dependent and decreases with the development of strains, then the strain rate will have to increase to balance Equation (3).

Finally, in this conjecture, the “tertiary” creep may also occur by any combination of the factors explained above.

Prediction of Creep

It can be shown that Equations (2) and (3) are the differential equations for the creep process. It can also be shown that these equations are non-linear and an analytical solution is very difficult (if not impossible) to obtain. Therefore, a numerical procedure is required for predicting creep. Referring to Equation (3), with the knowledge of the frictional and viscous resistances, for a given applied deviatoric stress, σ_d , there is a relationship between the shear strain and strain rate. This relationship can be better seen by re-arranging Equation (3) as follows:

$$\dot{\epsilon} = \left\{ \frac{[\sigma_d - \sigma_{df}(\epsilon)]}{K} \right\}^{1/n} \quad (4)$$

Equation (4) allows the construction of a plot for the relationship between the inverse of the strain rate and the shear strain for a given applied deviatoric stress, as the one below:

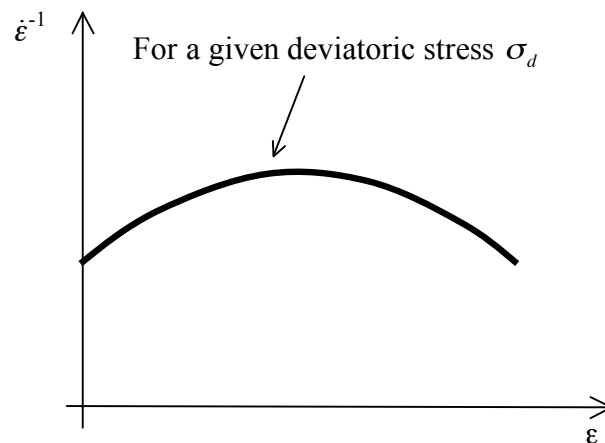


Figure 3 – Relationship between strain rate and strain for a given deviatoric stress in a creep test.

Therefore, the expression for the computation of time is equal to the area between the curve and the

horizontal axis in Figure 3. That is:

$$t(\varepsilon) = \int_0^\varepsilon \left(\frac{d\varepsilon}{dt} \right)^{-1} d\varepsilon \quad (5)$$

Equations (3) to (5) are valid for any stage of creep, as according to Martins' model, no significant difference exists between what is arbitrarily considered "primary", "secondary" (or steady-state) or "tertiary" creep. Creep is, according to the model, the transference that occurs between viscous and frictional resistances.

Although an analytical solution for Equations (2) or (3) may never be obtained, one particular case of interest may be solved. Referring to Equation (3) and considering a specified stress range, the frictional deviatoric stress may be considered linearly proportional to the shear strains (although not necessarily implying elastic behavior), and the following differential equation can be written:

$$\sigma_d = E \cdot \varepsilon + K \cdot \dot{\varepsilon}^n \quad (6)$$

Equation (6) is similar to Kelvin-Voigt's rheological model, although the viscosity function is non-linear. The solution of Equation (6) and the expression of the variation of the strain rate with time are presented below.

$$\varepsilon = \left(\frac{\sigma_d}{E} \right) - \left(\frac{K}{E} \right) \cdot \frac{1}{\left[\left(\frac{K}{\sigma_d} \right)^{\left(\frac{1-n}{n} \right)} + \left(\frac{1-n}{n} \right) \frac{E \cdot t}{K} \right]^{\left(\frac{n}{1-n} \right)}} \quad (7)$$

$$\dot{\varepsilon} = \frac{1}{\left[\left(\frac{K}{\sigma_d} \right)^{\left(\frac{1-n}{n} \right)} + \left(\frac{1-n}{n} \right) \cdot \frac{E \cdot t}{K} \right]^{\left(\frac{1}{1-n} \right)}} \quad (8)$$

Referring to Equation (7), it can be seen that for $t = 0$, $\varepsilon = 0$, and for $t \rightarrow \infty$ the strain is equal to $\varepsilon = \sigma_d / E$. In addition, considering Equation (8), it can be shown that, after applying log to both sides of the equation, an approximate linear relationship (apart from the very beginning of the creep process) between $\log(\dot{\varepsilon})$ and $\log(t)$ exists as shown on Figure 4 below. The slope of this curve is, according to the equation, equal to $-1/(1-n)$.

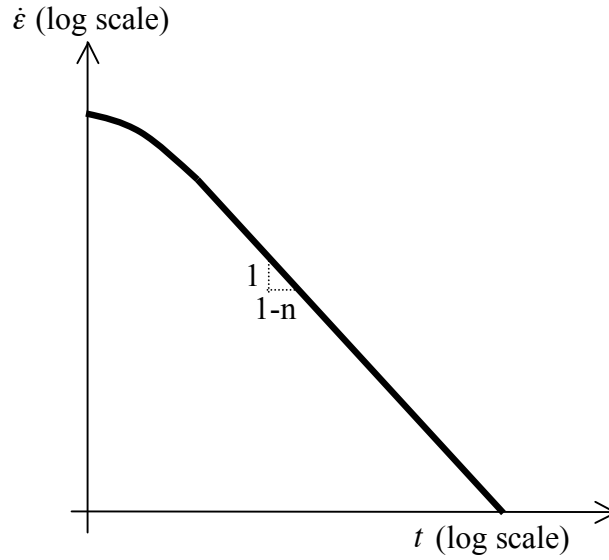


Figure 4 – Relationship between the strain rate and time in a bi-log scale.

Although, strictly speaking, Equations 6 to 8 can be applied only for “primary” creep for a stress range where E can be considered constant, it can be shown that it may be considered as an approximation for the entire process by considering different E 's by parts and according to stress range.

Vaid and Campanella (1977) also carried out Constant Load Tests on the Haney. As it will be shown in the next section, these tests can be analyzed in a similar fashion as the creep tests. For developing the numerical procedure and the analytical solution for the constant load tests it is only necessary to account for the decrease in the applied initial deviatoric stress during the test as a function of the shear strain.

Prediction of Constant Load Tests

A Constant Load Test is similar to a Creep Test, but, instead of maintaining the deviatoric stress constant during the entire test, a deviatoric load is held constant. Due to Poisson's effect, as the deformation of the specimen progress with time under constant loading, the cross section of the specimen (subjected to compressive loads) increases and therefore decreasing the initial deviatoric stress. Referring to Equation (3) and considering that the Poisson ratio in an undrained test for a saturated soil is 0.5, it follows that:

$$\sigma_d = \sigma_{d_0} \cdot (1 - \varepsilon) = \sigma_{df}(\varepsilon) + K \cdot \dot{\varepsilon}^n \quad (9)$$

Similarly to what was done in the numerical procedure for the Creep Tests, Equation (9) can also be re-arranged to show explicitly the relationship between strain rate and shear strain for a given initial deviatoric stress, σ_{d_0} . This relationship is:

$$\dot{\varepsilon} = \left\{ \frac{[\sigma_{d_0} \cdot (1 - \varepsilon) - \sigma_{df}(\varepsilon)]}{K} \right\}^{1/n} \quad (10)$$

In a similar fashion, Equation (5) can be used to calculate time required for a specimen subjected to a given initial deviatoric stress to achieve a certain strain, ε .

Referring to Equation (9) and again assuming that the frictional deviatoric stress is linearly proportional to the strain (although not necessarily implying elastic behavior) the following equation can be written:

$$\sigma_d \cdot (1 - \varepsilon) = E \cdot \varepsilon + K \cdot \dot{\varepsilon}^n \quad (11)$$

The solution for differential equation (11) and the expression of strain rate are as follows:

$$\varepsilon = \left(\frac{\sigma_{d_0}}{\sigma_{d_0} + E} \right) - \left(\frac{K}{\sigma_{d_0} + E} \right) \cdot \frac{1}{\left[\left(\frac{K}{\sigma_{d_0}} \right)^{\left(\frac{1-n}{n} \right)} + \left(\frac{1-n}{n} \right) \frac{(\sigma_{d_0} + E) \cdot t}{K} \right]^{\left(\frac{n}{1-n} \right)}} \quad (12)$$

$$\dot{\varepsilon} = \frac{1}{\left[\left(\frac{K}{\sigma_{d_0}} \right)^{\left(\frac{1-n}{n} \right)} + \left(\frac{1-n}{n} \right) \cdot \frac{(\sigma_{d_0} + E) \cdot t}{K} \right]^{\left(\frac{1}{1-n} \right)}} \quad (13)$$

It can be seen from Equation (12), that for $t = 0$, $\varepsilon = 0$, and for $t \rightarrow \infty$ the strain reaches $\varepsilon = \sigma_{d_0} / (\sigma_{d_0} + E)$. In addition, considering Equation (13), it can be shown that, after applying log to both sides of the equation, that an approximate linear relationship (apart from the very beginning of the creep process) between $\log(\dot{\varepsilon})$ and $\log(t)$ exists similar to the one represented in Figure 4.

Assessment of the Parameters of the Model

According to Vaid and Campanella (1977), “Haney Clay is believed to have been deposited in a marine environment and later subjected to partial leaching due to surface infiltration. It is a grey silty clay with liquid limit = 44%, plastic limit = 26%, maximum past pressure of about 3.5 kg/cm² (340 kPa) and a sensitivity from 6 to 10”.

Majority of the laboratory tests undertaken by Vaid and Campanella (1977) were normally consolidated hydrostatically to 515 kPa. After consolidation, the specimens were left resting in an undrained condition for 12 hours under the consolidation pressures prior to shear loading. According to Vaid and Campanella (1977), the pore-pressure generated during this undrained period was attributed to the arrest of secondary consolidation. All measurements were done electronically and all data were automatically recorded on a digital magnetic tape using a high speed (10 channels per second) Vidar Digital Data Acquisition System. In addition, the test program was carried out in a constant temperature environment with a maximum temperature variation of $\pm 0.25^\circ \text{C}$.

According to Vaid (2004), the tests were not carried out with internal load cells and did not use the “free-ends” technique to minimize friction between the specimens and the top cap and pedestal. Instead, an external load cell with a specially designed continuously air leaking seal was used. According to Vaid (2004), the maximum friction in the air seal on the loading ram was 10 grams, and was independent of the cell pressure.

The experimental results of the Constant Rate of Strain Tests were used for deriving parameters of the Modified Martins’ Model (the frictional and the viscous resistances) in order to allow for the predictions of the undrained creep and constant load tests and are reproduced below.

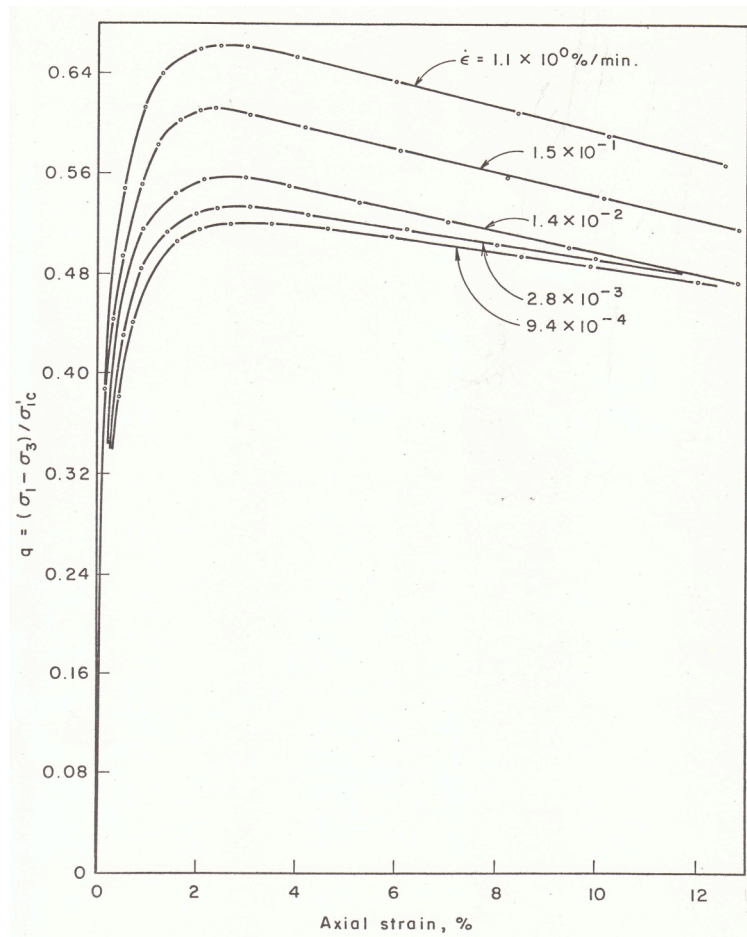
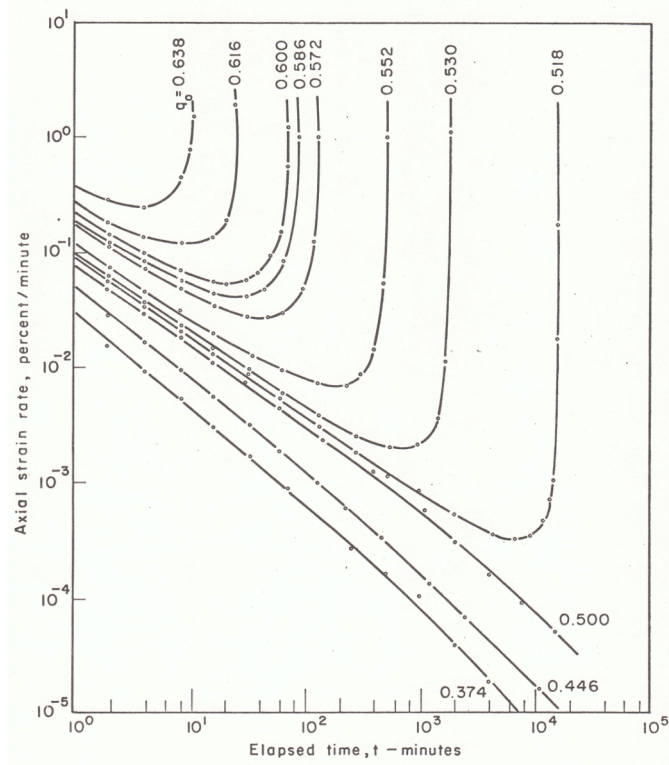
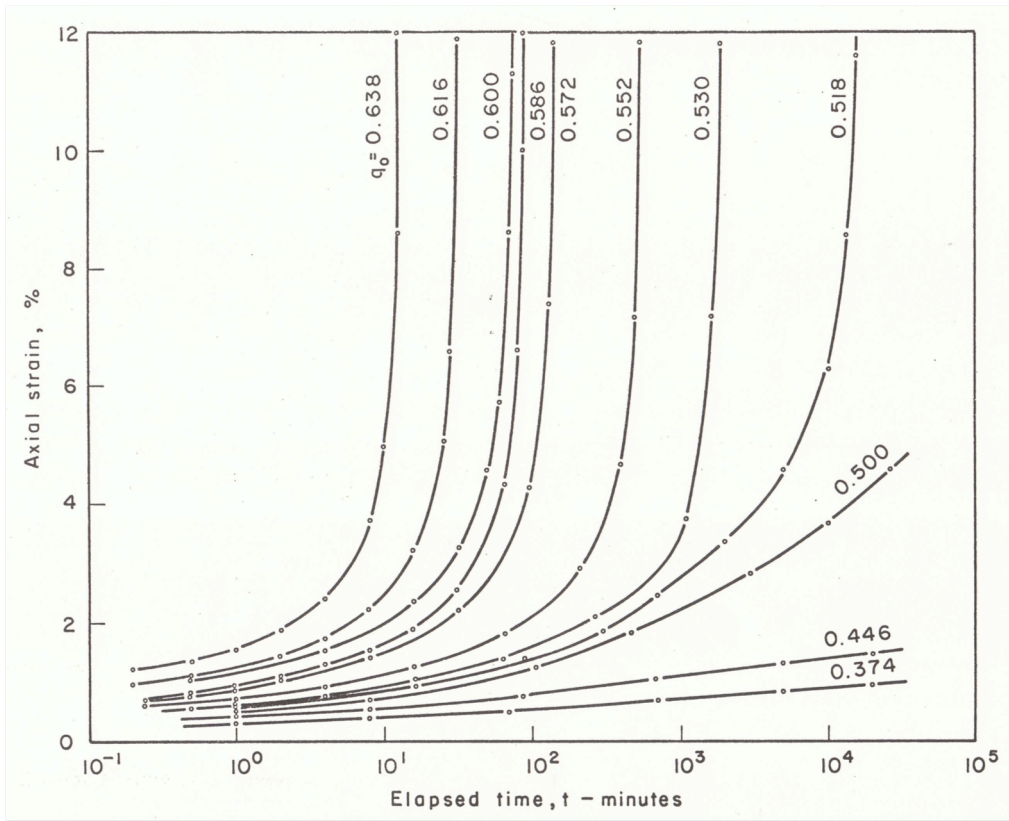
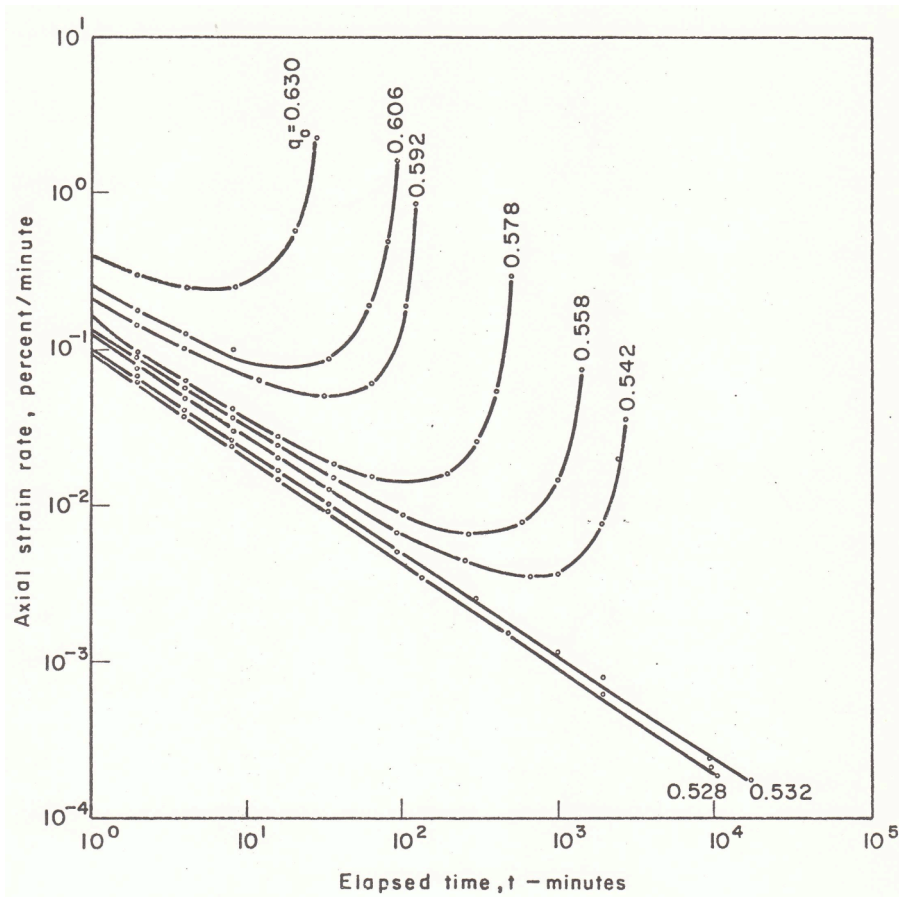
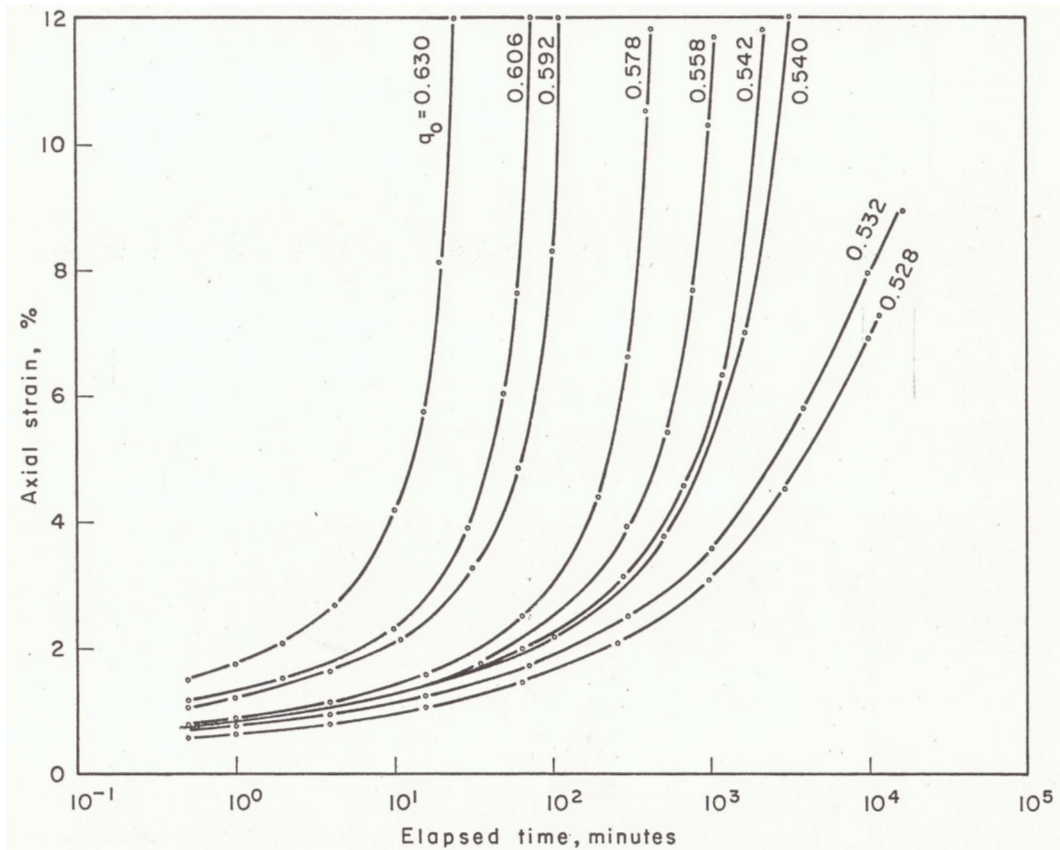


Figure 5 – Constant rate of Strain Test carried out by Vaid and Campanella (1977)



Figures 6 and 7 – Creep Tests carried out by Vaid and Campanella (1977).



Figures 8 and 9 – Constant Load Tests carried out by Vaid and Campanella (1977)

According to the model developed by Martins the viscous resistance in a Constant Rate of Strain test is instantaneously mobilized at the beginning of the test and remains constant thereafter. This effect can be seen both on a deviatoric stress vs strain plot as well as on an effective stress path plot.

The best procedure for assessing the viscous resistance, if possible, is by using both plots. The assessment of the viscous resistance using only the deviatoric stress vs strain plots is very difficult as it involves the assessment of deviatoric stress for very small strains, and may lead to apparent discrepancies in the assessed viscous resistance, if not used together with the stress path plots.

As pore-pressure measurements of the tests were not available, the assessment of the viscous resistances of the Constant Rate of Strain tests could only be carried out using the deviatoric stress x strain plot. However, as this assessment led to apparent discrepancies, another procedure was developed.

First, the viscous resistance from the test with the highest strain rate was assessed, as it possesses the highest viscous resistance. The viscous resistance for the test with the strain rate of 1.1%/min, when normalized with respect to the consolidation pressure, is about 0.2. However, because of the reasons explained above, it could be greater or smaller than this value.

Subtracting the viscous resistance from the deviatoric stress curve of the test with the strain rate of 1.1%/min, the frictional resistance curve was assessed. The Figure below presents the frictional resistance for the test with a strain rate of 1.1 %/min.

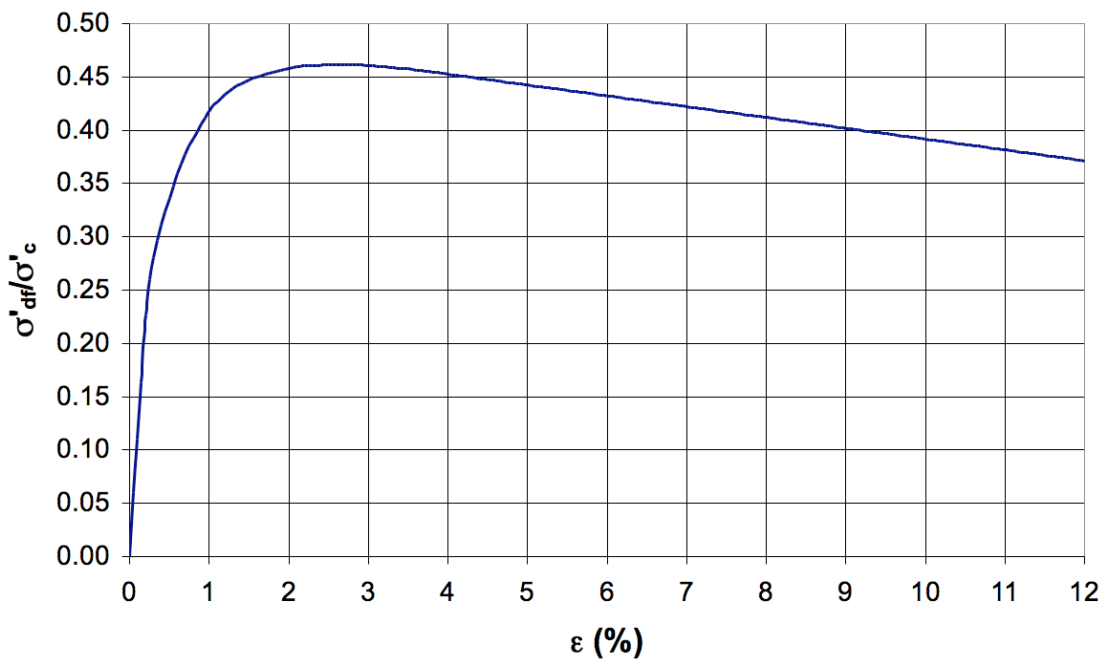


Figure 10 – Frictional resistance curve from the Constant Rate of Strain test with strain rate = 1.1 %/min.

Having assessed the frictional resistance curve from this test, the viscous resistances of the other tests were assessed by subtracting, for a given strain, the frictional deviatoric resistance for that strain from the deviatoric stress at the same strain. For a strain of 2.5%, the normalized frictional resistance is about 0.46. Subtracting this frictional resistance from the deviatoric stresses of the other tests for the same strain, the following viscous resistance were obtained:

$\dot{\epsilon}$ (%/min)	$2V/\sigma'_c$
1.5×10^{-1}	0.15
1.4×10^{-2}	0.09
2.8×10^{-3}	0.07
9.4×10^{-4}	0.06

Table 1 – Normalized viscous resistances and respective strain rates.

The following plot shows the pairs of values of strain rate and normalized viscous resistances, $2V/\sigma'_c$, as well as a power function of the strain rate fitting the data.

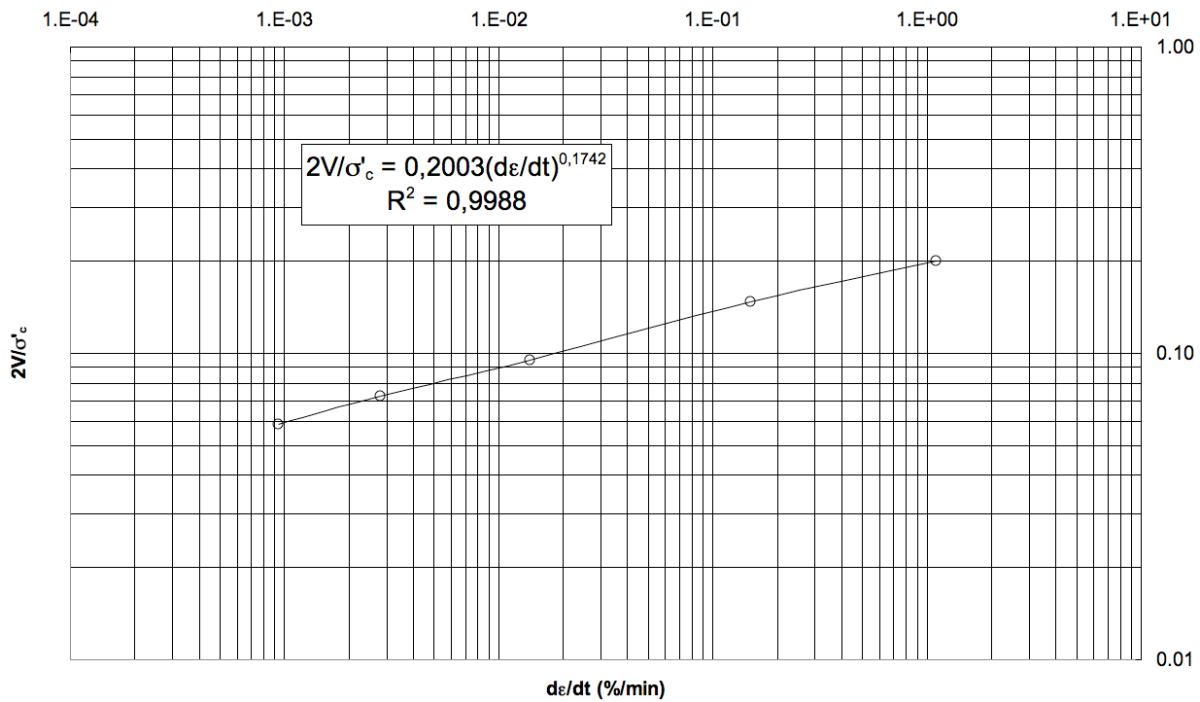


Figure 11 – Assessment of the viscous resistance function.

Where $2V = \sigma'_{dv}$ is the viscous deviatoric stress.

By assessing the viscous resistances for all the other tests, the frictional resistance for each test can be assessed. This can be done by subtracting the assessed viscous resistance from the deviatoric curves for each one of the other tests. Figure 2 shows the frictional resistances of all tests as well as a curve representing the average deviatoric stress vs strain curve.

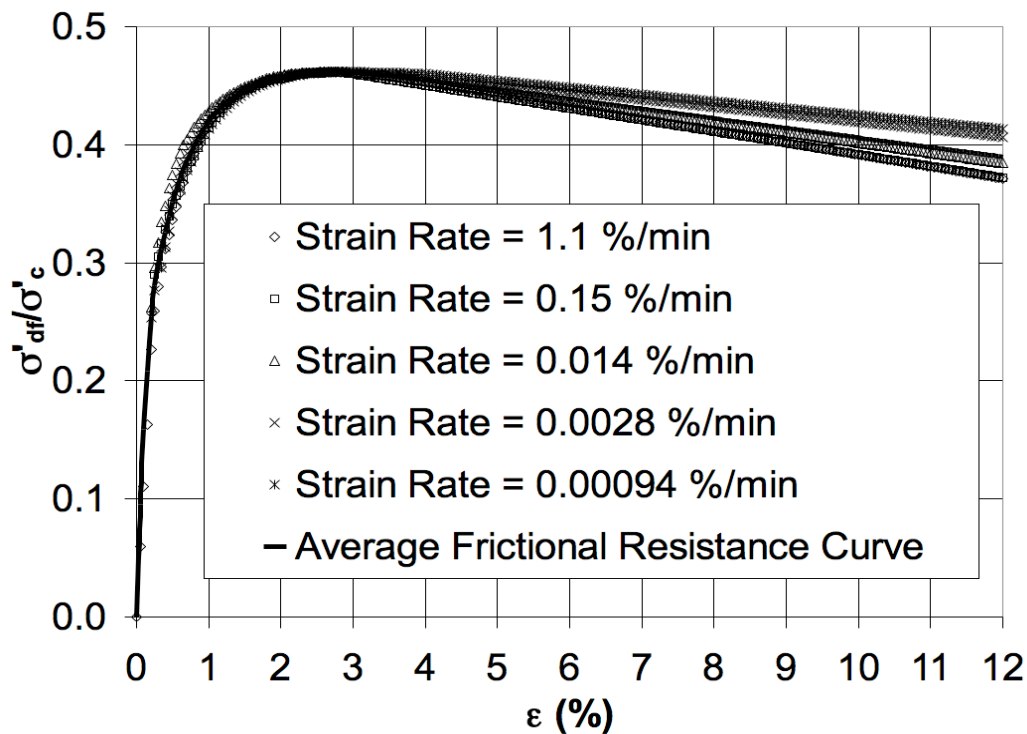


Figure 12 – Assessment of the normalized frictional resistance curves.

It is worth noting that, because the test results are normalized in relation to the consolidation pressures, both the assessed viscous and frictional resistances are also normalized with respect to the consolidation pressure. This normalization, however, does not make the analysis invalid, as according to Martins's model, the normalizing behavior is one of the hypotheses.

Finally, it is also worth mentioning that the maximum frictional resistance, 0.46, assessed above, is consistent with the upper yielding strength concept from Finn and Snead (1973). Although close, this value differs from the upper yielding value suggested by Vaid and Campanella (1977). For Vaid and Campanella (1977), the upper yielding would be between 0.5, which is the creep test that did not fail within 3 weeks, and 0.518, which is the creep test that did fail.

Check of the Assessed Parameters

Using Dimensional Analysis

Dimensional analysis is frequently used for providing guidance for the conception, construction, execution and interpretation of physical models. In this work, the tests carried out by Vaid and Campanella (1977) can be considered the physical models and therefore dimensional analysis was used to assess the consistency of the parameters of the model. The basis of the theory will not be presented here but can be found on Vaschy (1890), Buckingham (1915), Bridgman (1922), Langhaar (1965) and Carneiro (1993),

By using the Theorem of Vaschy-Buckingham, the dimensional matrix of the time-dependent strength problem was assembled and the following Π numbers were obtained:

$$\Pi_1 = \frac{\sigma_d}{\sigma_{df\ max}} \quad \text{and} \quad \Pi_2 = t \cdot \left(\frac{\sigma_{df\ max}}{K} \right)^{1/n}$$

Therefore, if the physical understanding of the process is correct and if the parameters assessed are consistent, there must be a functional relationship between Π_1 and Π_2 . The following figure shows a plot of the two Π numbers assessed above for the Constant Rate of Strain, Undrained Creep and Constant Load Tests for a strain of 2.5%.

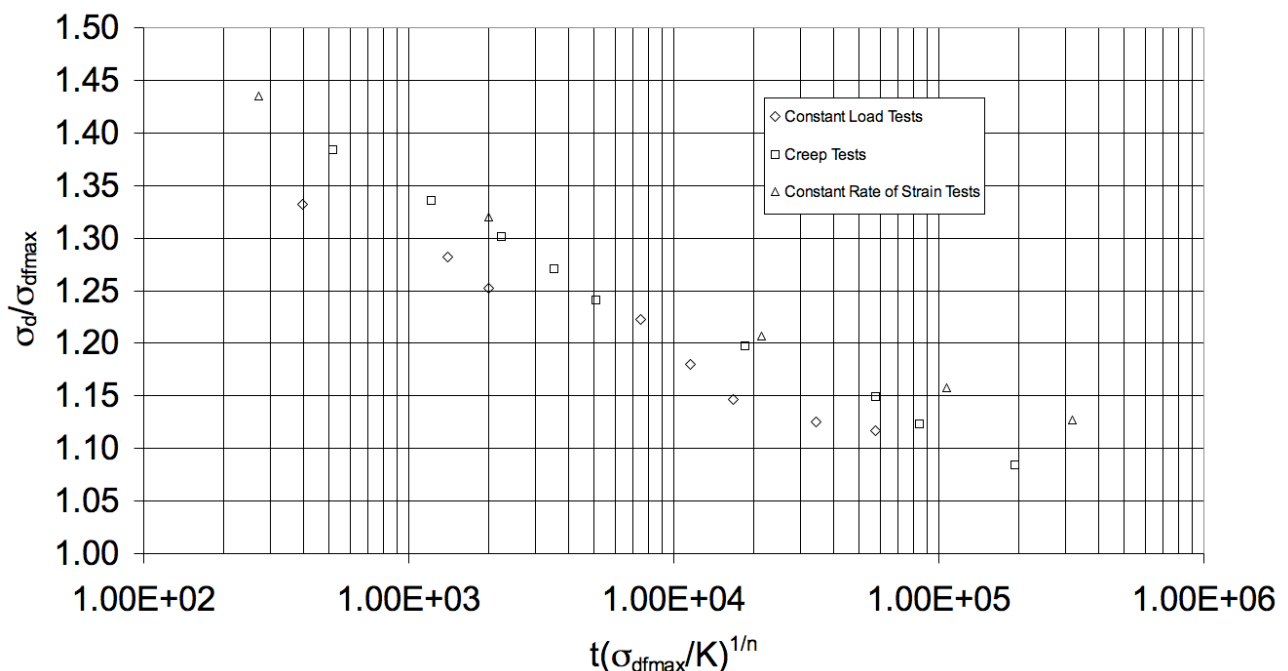


Figure 13 – Dimensional Analysis of the Time-Dependent Strength for the Haney Clay.

Numerical Verification

Equations (3) and (11) can be re-arranged to the following formats:

$$\frac{\sigma_{df}(\varepsilon) + K \cdot \dot{\varepsilon}^n}{\sigma_d} = 1 \quad (14)$$

$$\frac{\sigma_{df}(\varepsilon) + K \cdot \dot{\varepsilon}^n}{\sigma_{d_0} \cdot (1 - \varepsilon)} = 1 \quad (15)$$

Using the re-arranged equations above, the consistency of the assessed parameters can be checked by using any point of the creep or constant load tests. Tables 2 and 3 below show the results of this numerical verification for the creep and constant load tests.

σ_d/σ'_c	Time (min)	$\varepsilon(\%)$	$d\varepsilon/dt$ (%/min)	σ_{df}/σ'_c	Equation (16)	Error (%)
0.638	1	1.58	3.70E-01	0.449	0.97	-3.19
0.638	5	2.72	2.78E-01	0.462	0.97	-2.54
0.616	1	1.26	2.78E-01	0.436	0.97	-3.23
0.616	20	3.87	2.41E-01	0.456	0.99	-0.62
0.6	5	1.65	8.43E-02	0.451	0.97	-3.22
0.6	60	5.72	2.86E-01	0.441	1.00	0.33
0.586	1	0.96	1.87E-01	0.415	0.96	-3.73
0.586	80	6.3	1.00E+00	0.436	1.09	8.57
0.572	5	1.28	5.99E-02	0.438	0.98	-1.93
0.572	50	2.73	2.86E-02	0.462	1.00	-0.47
0.552	1	0.74	1.22E-01	0.393	0.96	-3.62
0.552	500	7.62	1.00E+00	0.425	1.13	13.33
0.53	500	2.55	2.10E-03	0.461	1.00	-0.05
0.53	1000	3.5	2.30E-03	0.458	1.00	-0.41
0.518	2000	3.4	6.00E-04	0.459	0.99	-0.79
0.518	10000	6.38	4.00E-04	0.435	0.94	-6.11
0.5	400	1.8	1.10E-03	0.454	1.03	3.07
0.5	7000	3.44	1.00E-04	0.459	1.00	-0.23
0.446	1	0.44	5.05E-02	0.339	1.03	2.80
0.446	10000	1.41	2.00E-05	0.443	1.06	6.06
0.374	1	0.31	3.11E-02	0.300	1.09	9.39
0.374	4000	0.86	2.00E-05	0.404	1.16	16.23

Table 2 – Numerical verification for the creep tests.

σ'_{d0}/σ'_c	Time (min)	$\epsilon(\%)$	$d\epsilon/dt$ (%/min)	σ_{df}/σ'_c	Equation (17)	Error (%)
0.63	1	1.78	3.91E-01	0.454	1.01	0.86
0.63	10	4.22	2.75E-01	0.453	1.01	1.35
0.606	2	1.54	1.72E-01	0.448	1.00	-0.26
0.606	20	3.17	7.76E-02	0.460	1.00	0.21
0.592	3	1.57	1.13E-01	0.448	1.00	0.35
0.592	30	3.23	5.06E-02	0.460	1.01	0.95
0.578	10	1.45	3.55E-02	0.445	0.98	-2.33
0.578	100	3.05	1.43E-02	0.461	0.99	-0.82
0.558	50	2	1.24E-02	0.457	1.01	0.60
0.558	800	8.25	1.07E-02	0.420	0.99	-0.89
0.542	1000	5.72	3.80E-03	0.441	1.01	0.80
0.542	2000	10.74	8.90E-03	0.400	1.00	-0.36
0.532	1000	3.6	1.00E-03	0.458	1.01	0.84
0.532	10000	8.03	2.00E-04	0.422	0.95	-5.14
0.528	100	2.75	4.20E-03	0.462	1.05	4.83
0.528	10000	6.98	2.00E-04	0.430	0.96	-3.63
0.63	3	2.4	2.62E-01	0.461	1.01	0.68
0.606	40	5.05	1.03E-01	0.446	1.01	0.72
0.592	60	4.83	5.93E-02	0.448	1.01	0.98
0.578	400	10.71	5.77E-02	0.392	0.98	-1.57

Table 3 – Numerical verification for the Constant Load tests.

The numerical verification carried out in this section can be seen as similar to the one carried out by Vaid and Campanella (1977) for checking the validity of the equation $q = q(\epsilon, \dot{\epsilon})$.

Undrained Creep and Constant Load Test Predictions

Figures 14 to 52 shows the strain x time and strain rate x time plots for all the creep and constant load tests.

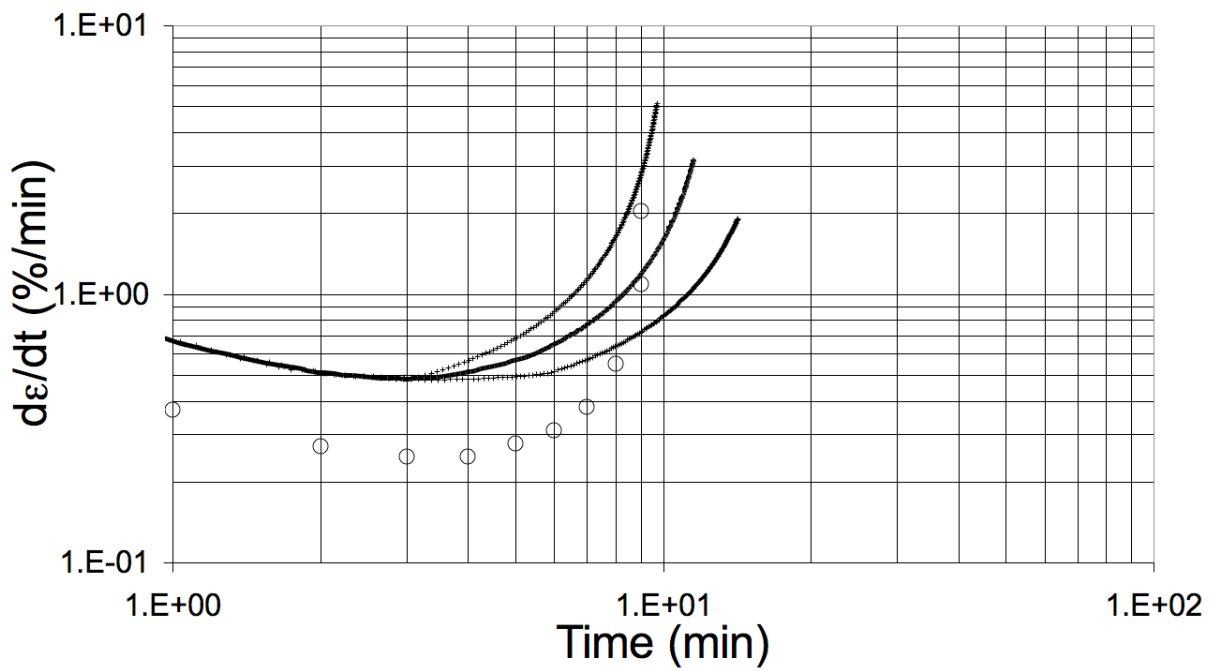
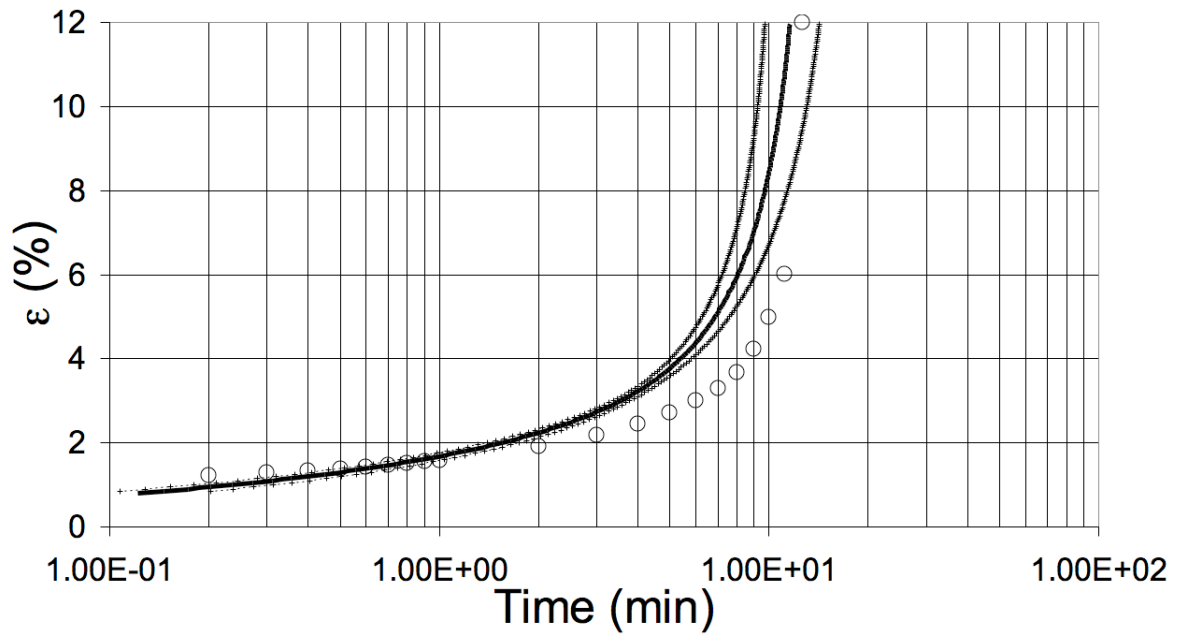
For carrying out the predictions of all the Figures (except Figures 32 to 35), the numerical procedures described in this paper were used. For integrating the areas below the inverse of the strain rate x strain curve (Figure 3) the method on the Trapezoids with a strain step of 0.05% was used.

The predictions carried out for Figures 32 to 35 were made using the analytical solution of the differential equation, Equations (7) and (8) with a different E every 0.05% strain interval.

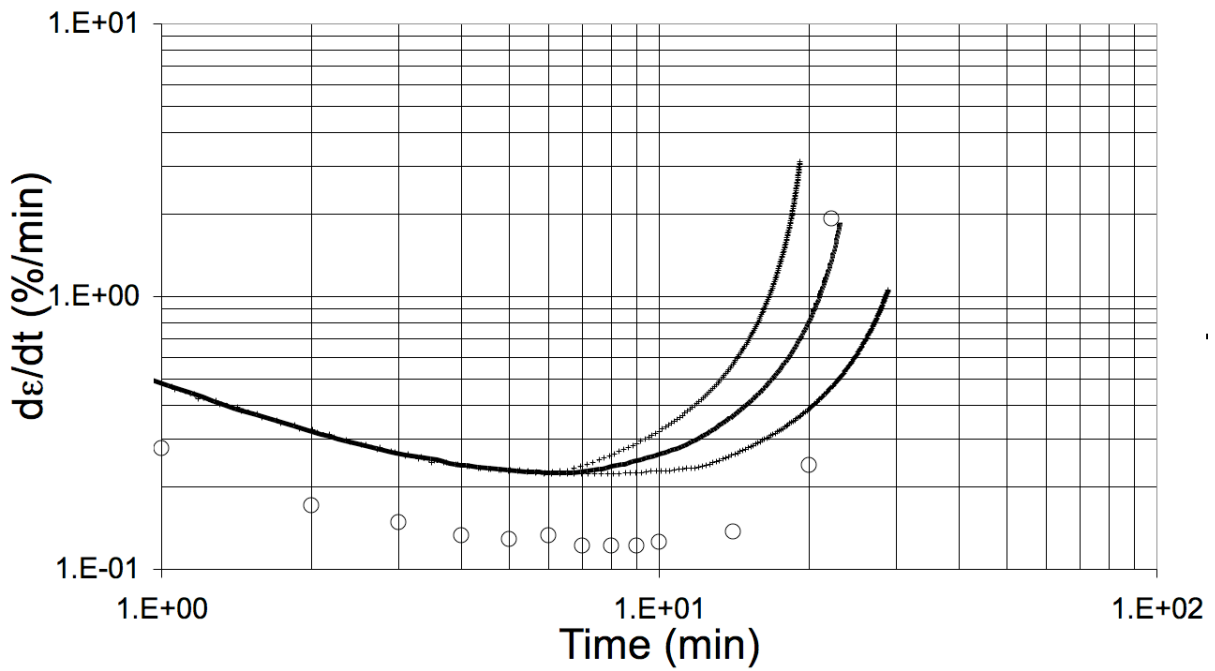
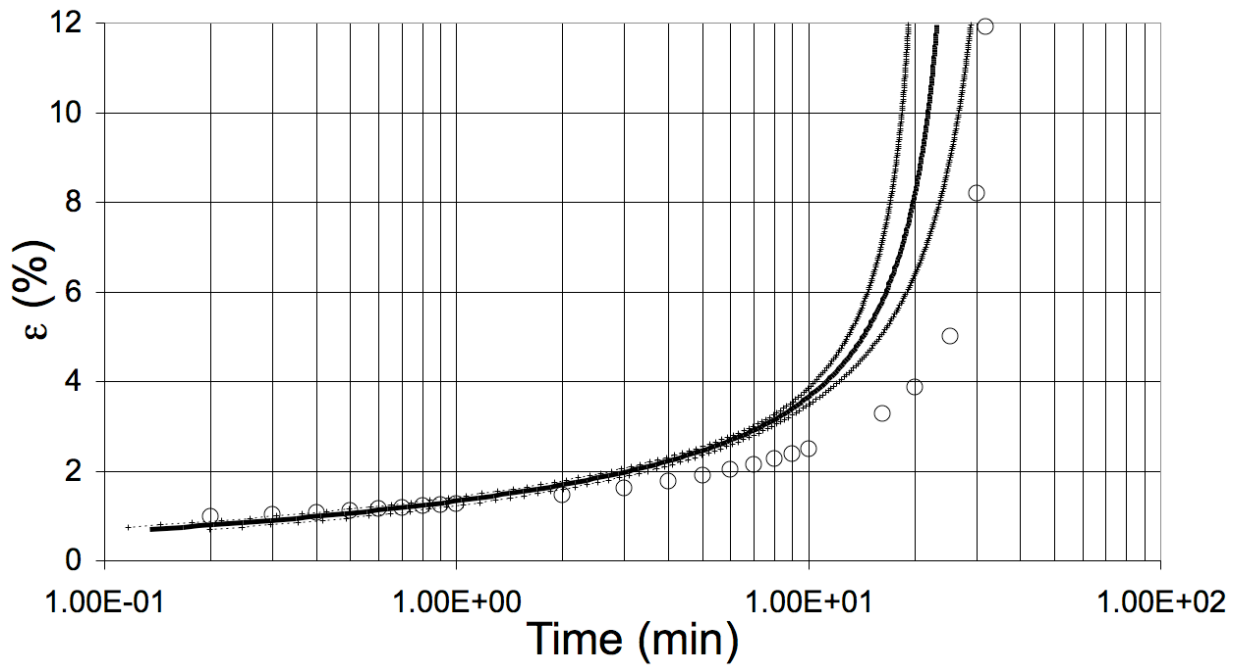
All predictions made use of the assessed viscous resistance function and three different frictional resistance curves. The frictional resistance curves used were the average curve (showed as a thick black solid line) and two other curves (showed as thin black dashed line with crosses) representing the upper and lower bounds of the frictional resistance data shown in Figure 12.

A discussion of the numerical sensitivity of the predictions is included in the discussion of the results.

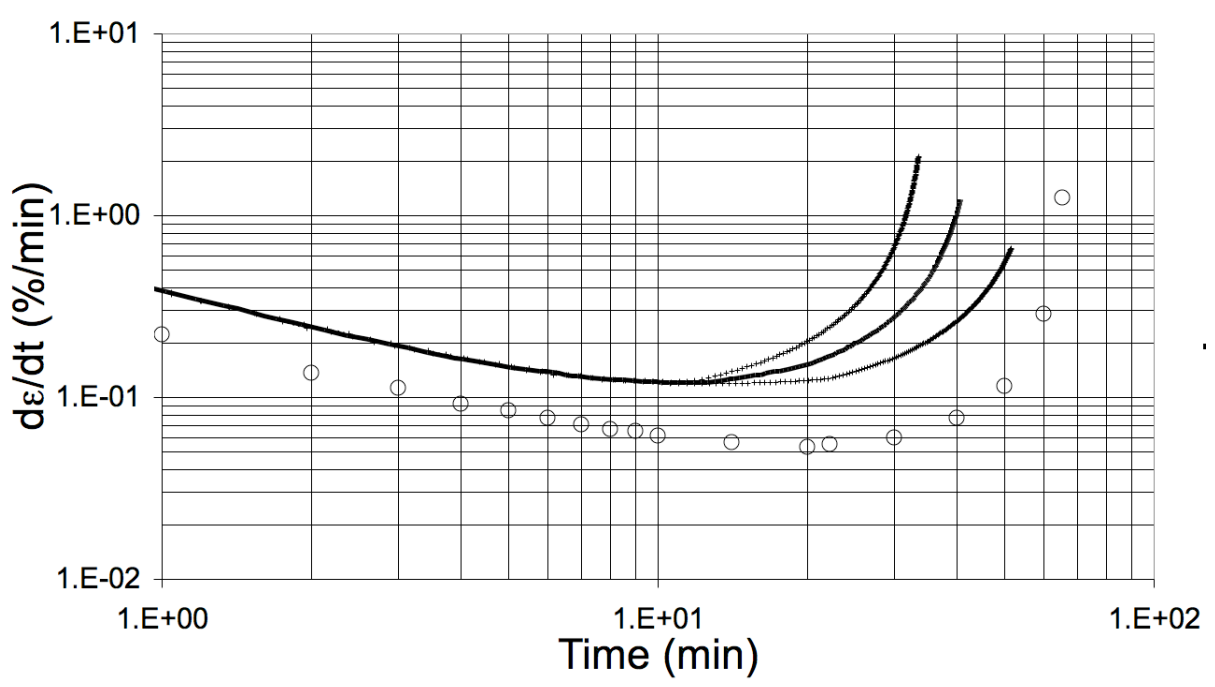
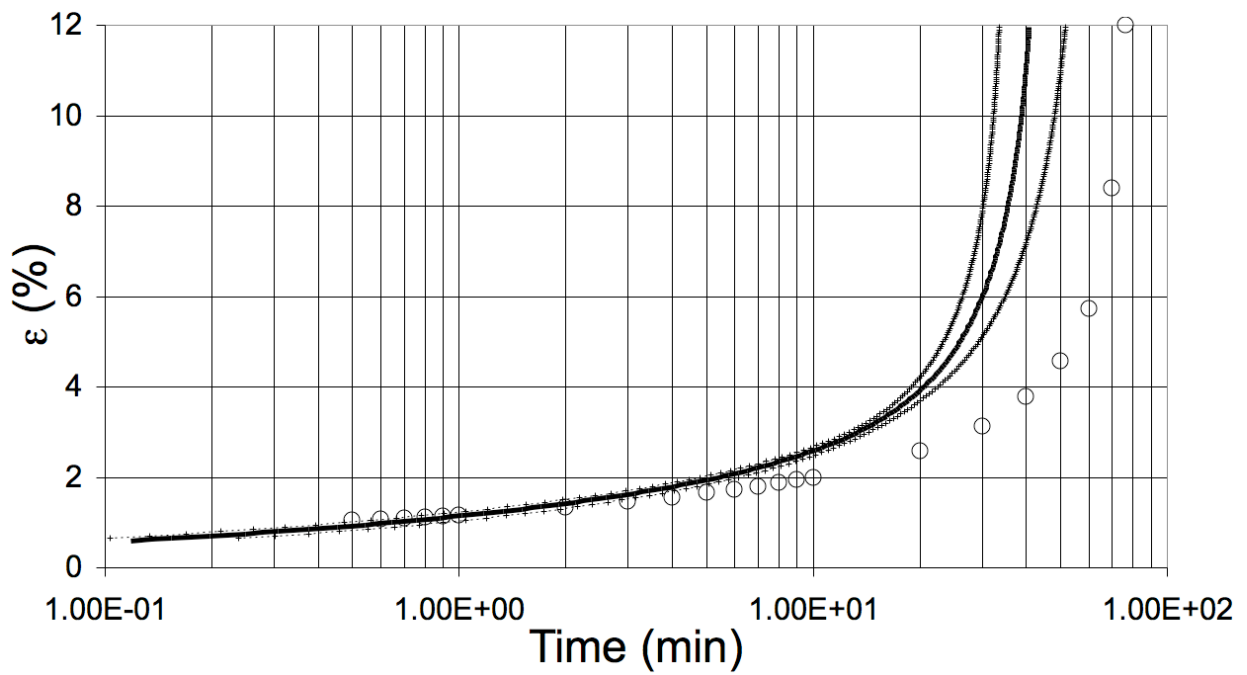
The tests data presented in the plots were obtained by interpolation of Figures 4, 5, 6 and 7 from Vaid and Campanella (1977).



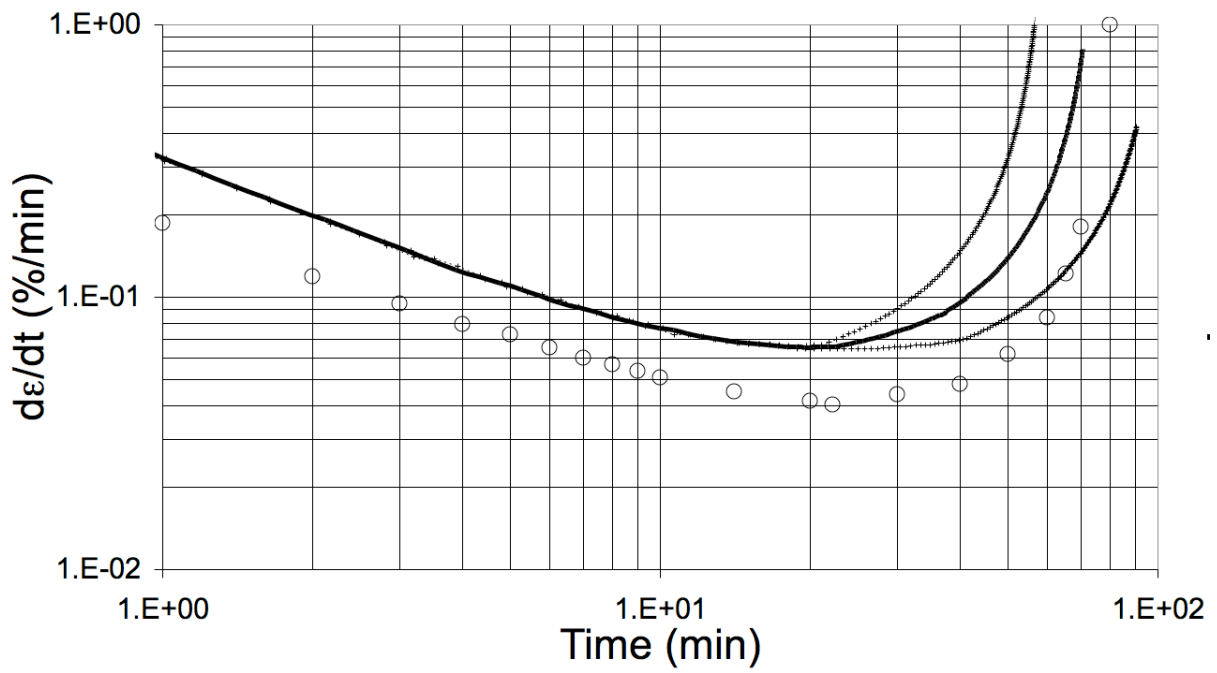
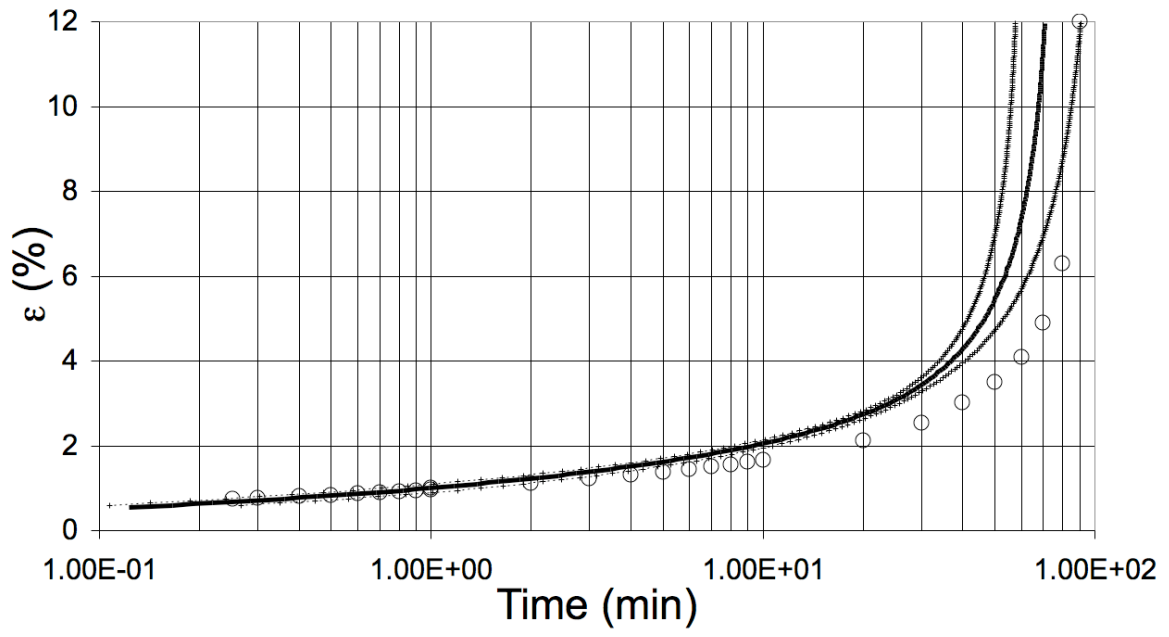
Figures 14 and 15 – Creep test - $\sigma_d/\sigma'_c = 0.638$



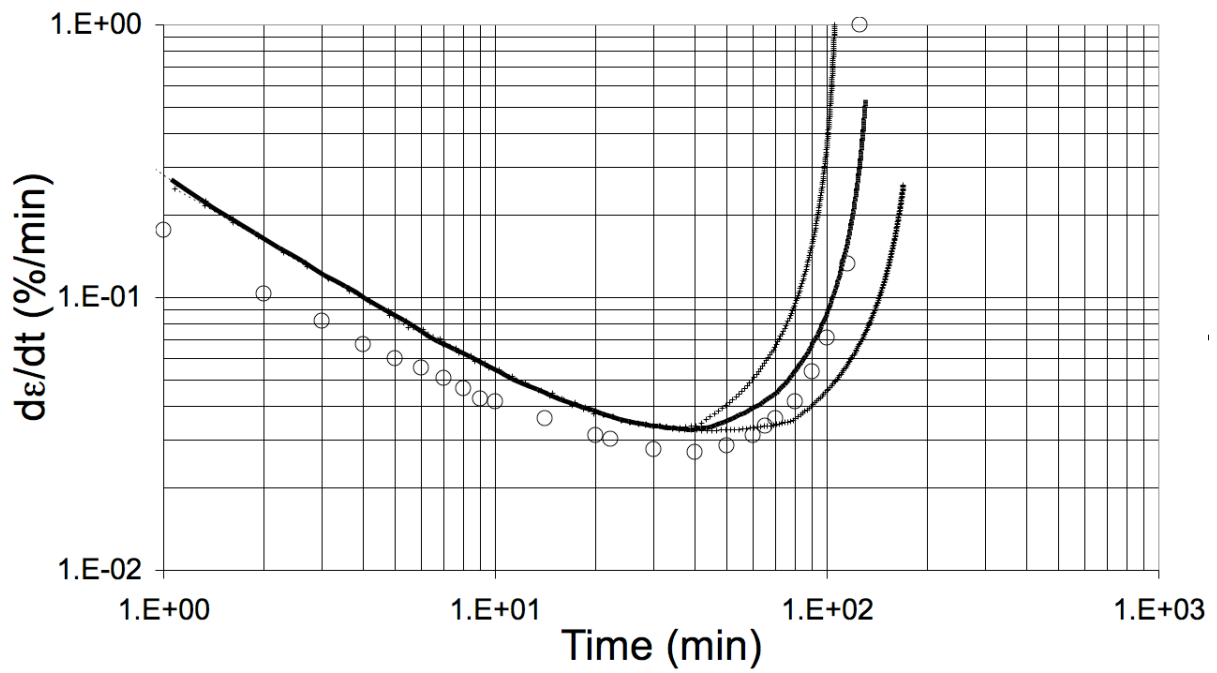
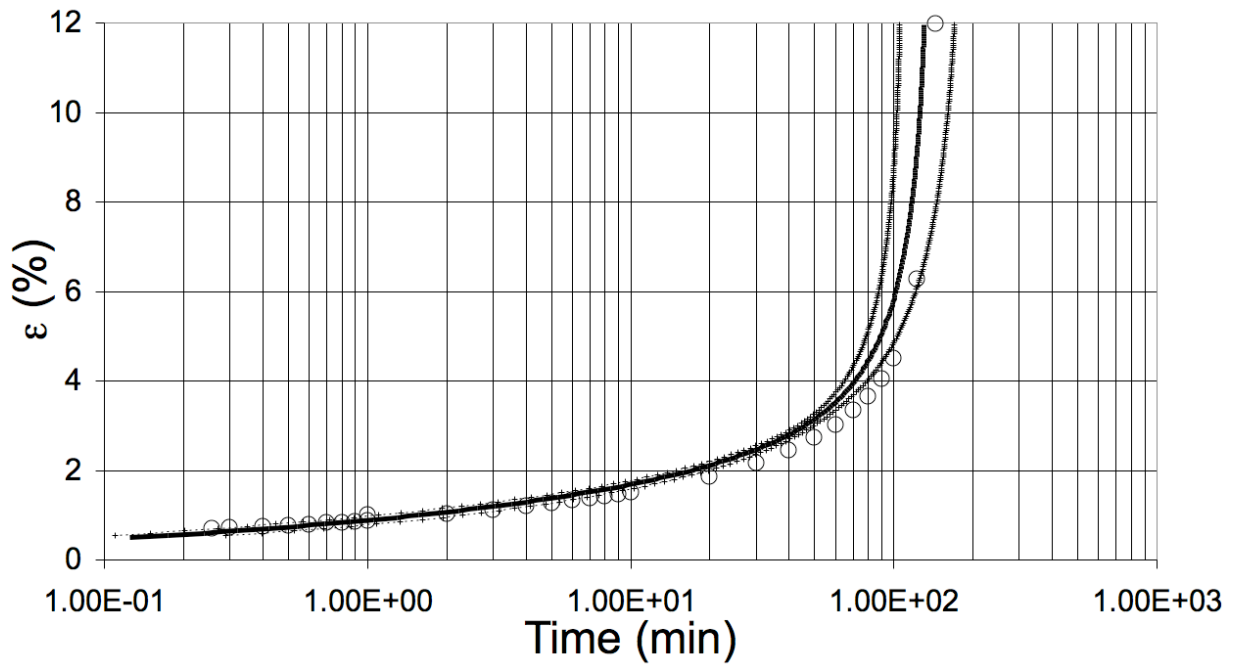
Figures 16 and 17 – Creep test - $\sigma_d/\sigma'_c = 0.616$



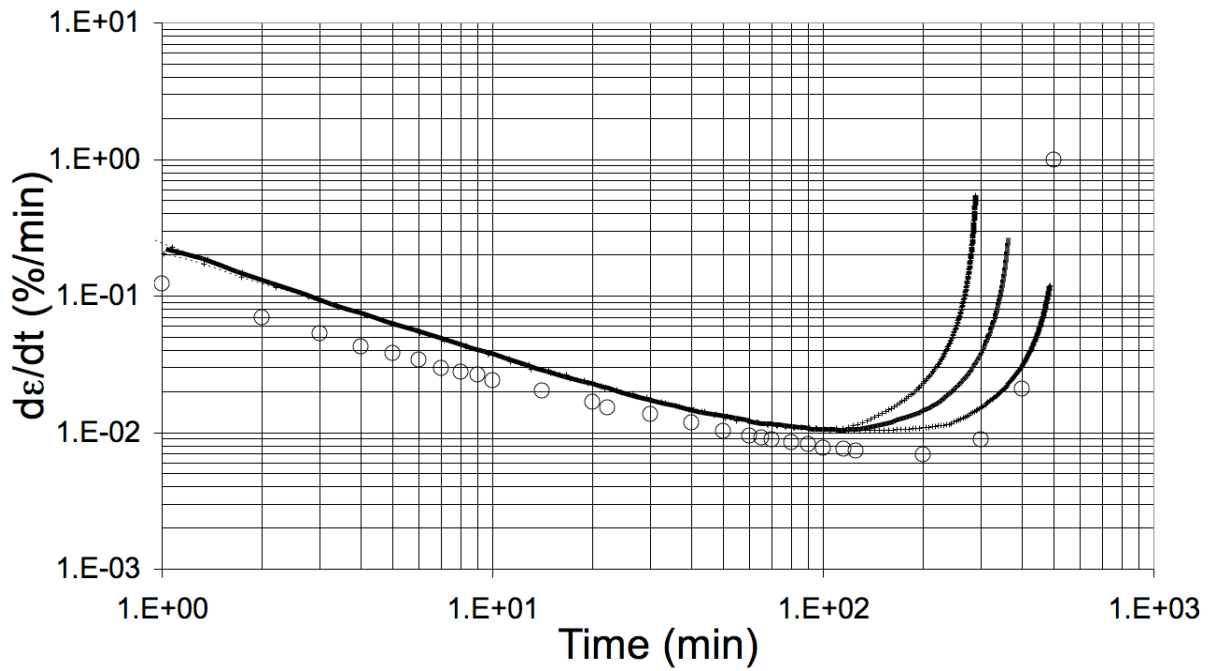
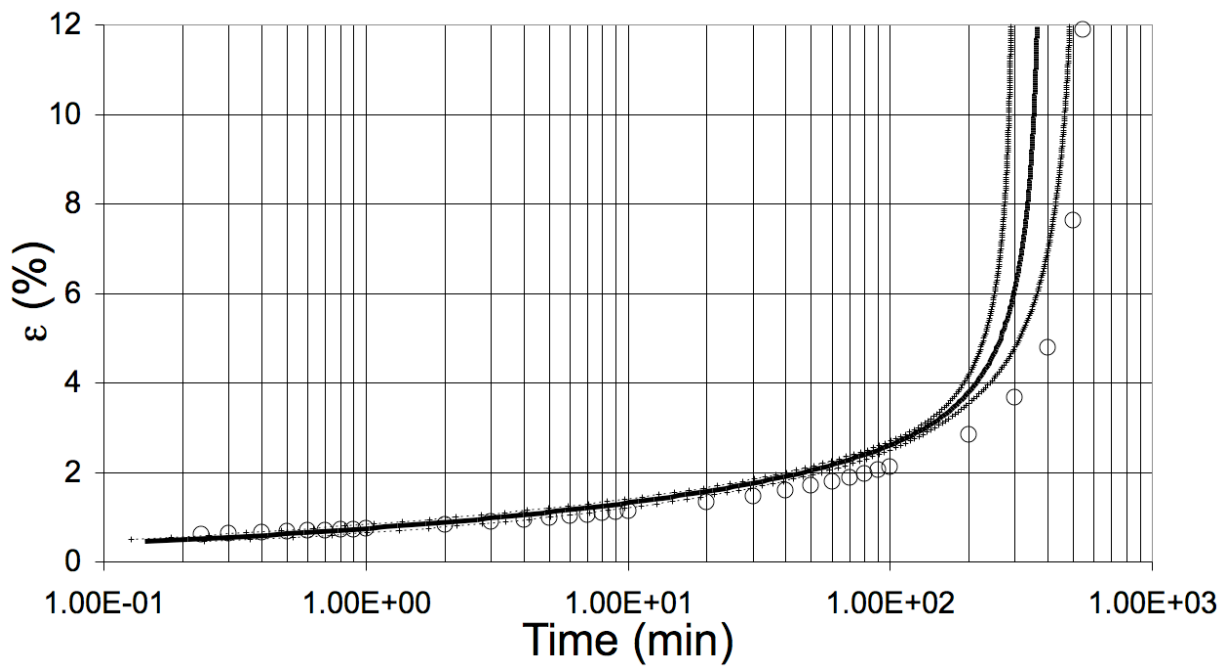
Figures 18 and 19 – Creep test - $\sigma_d/\sigma'_c = 0.600$



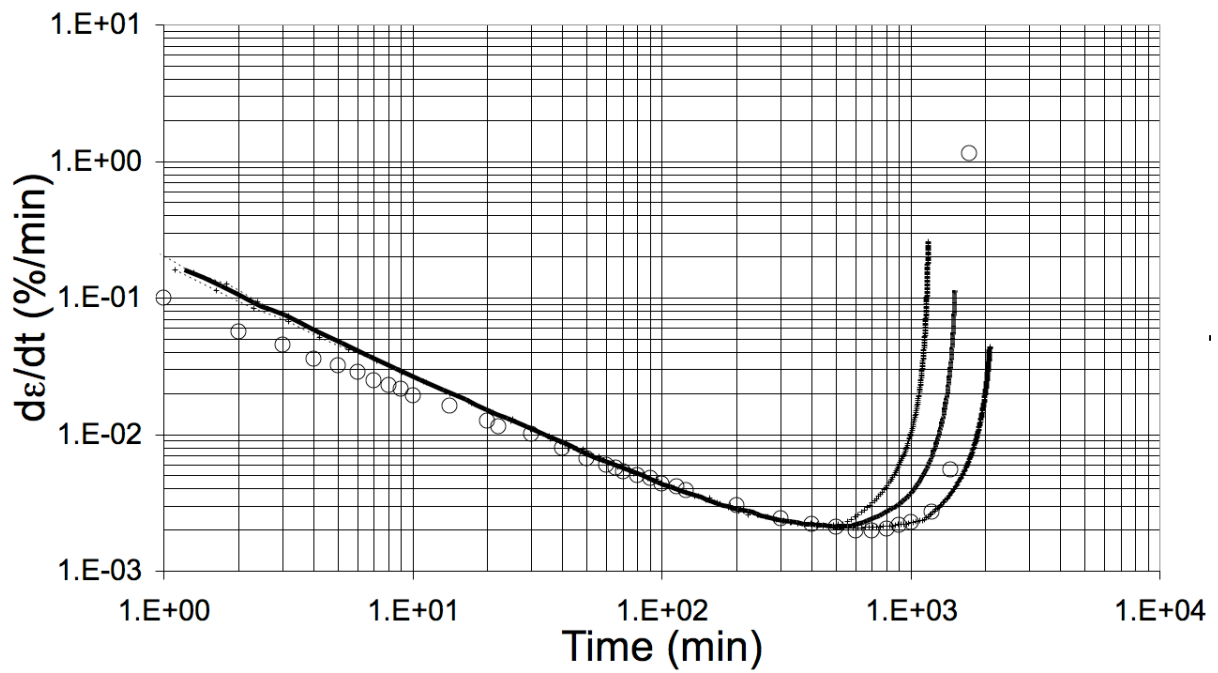
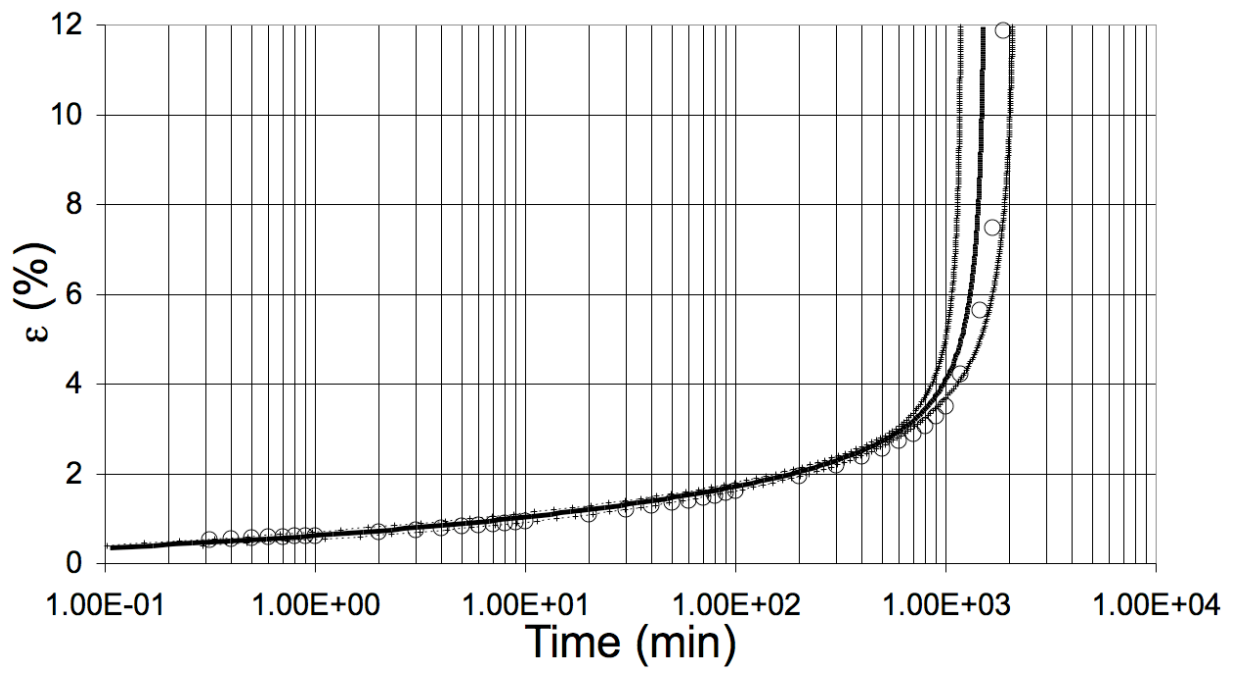
Figures 20 and 21 – Creep test - $\sigma_d/\sigma'_c = 0.586$



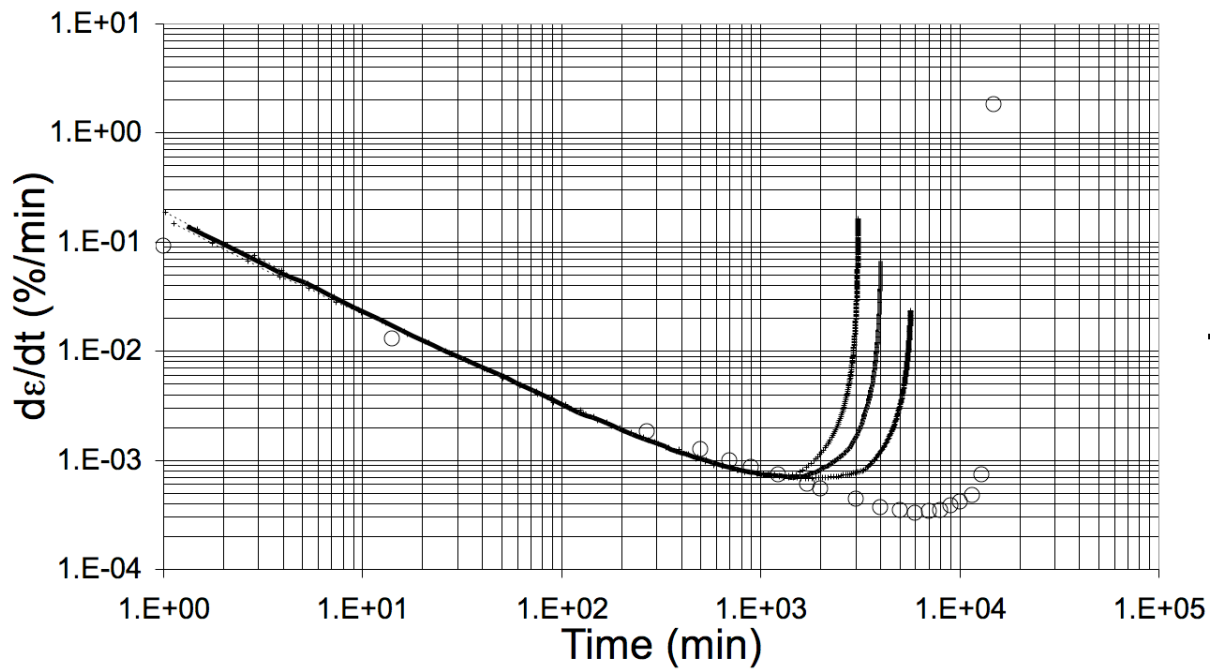
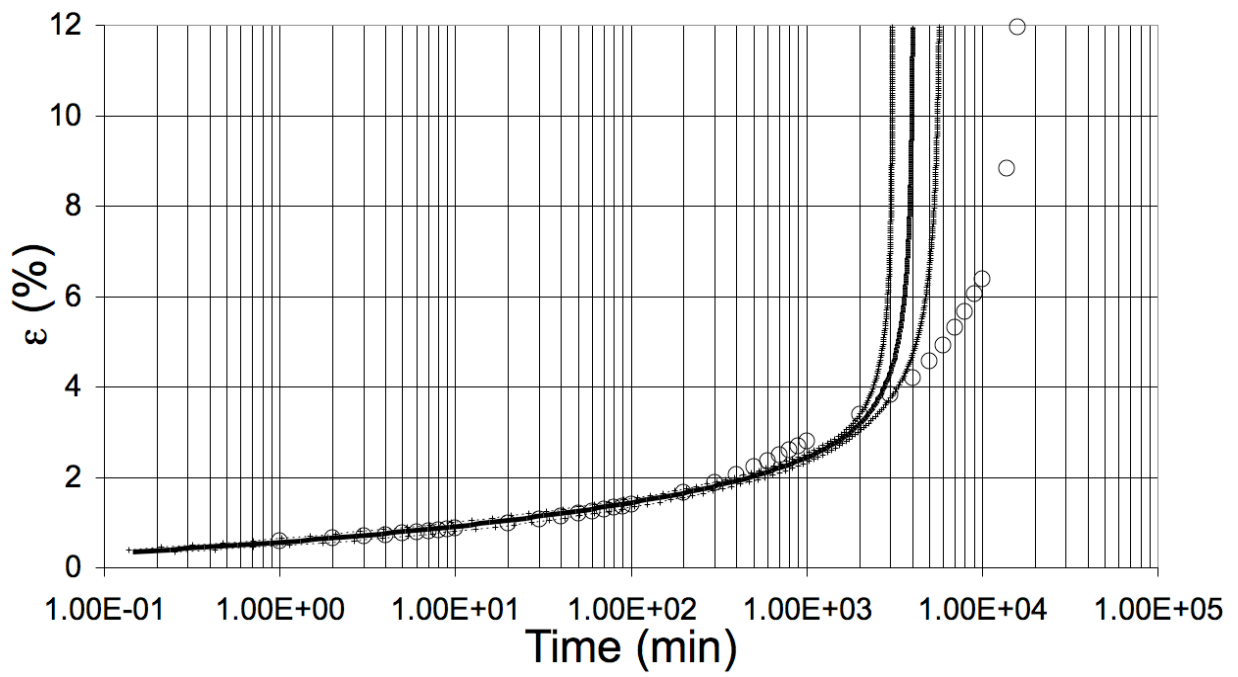
Figures 22 and 23 – Creep test - $\sigma_d/\sigma'_c = 0.572$



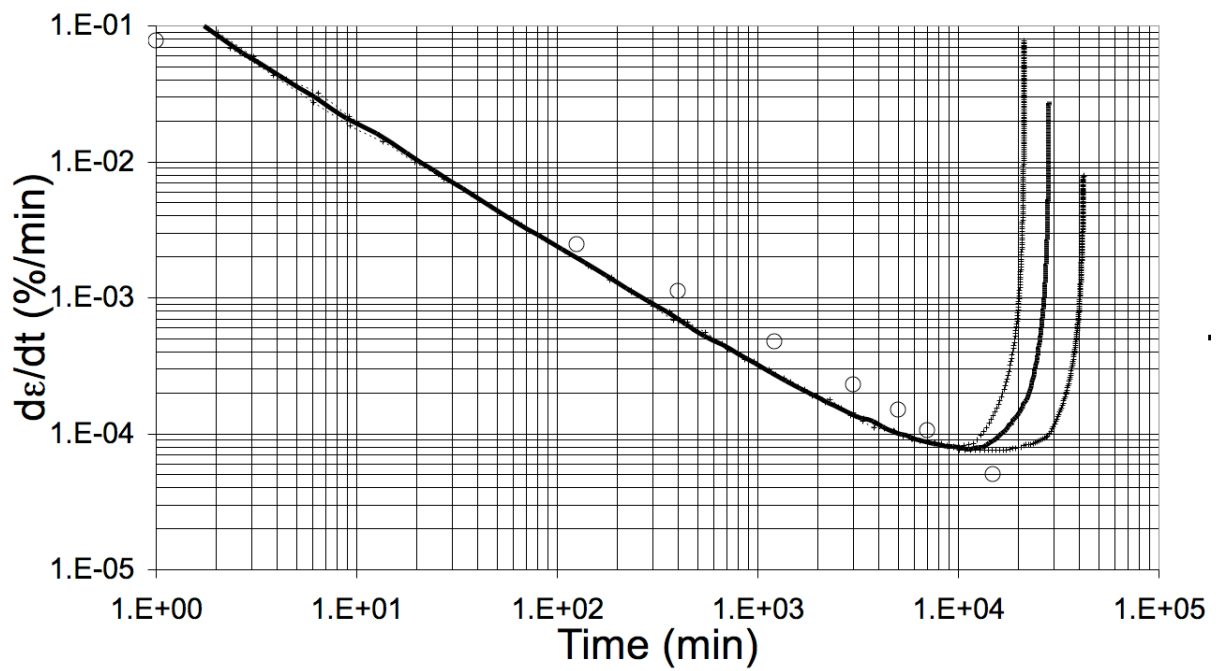
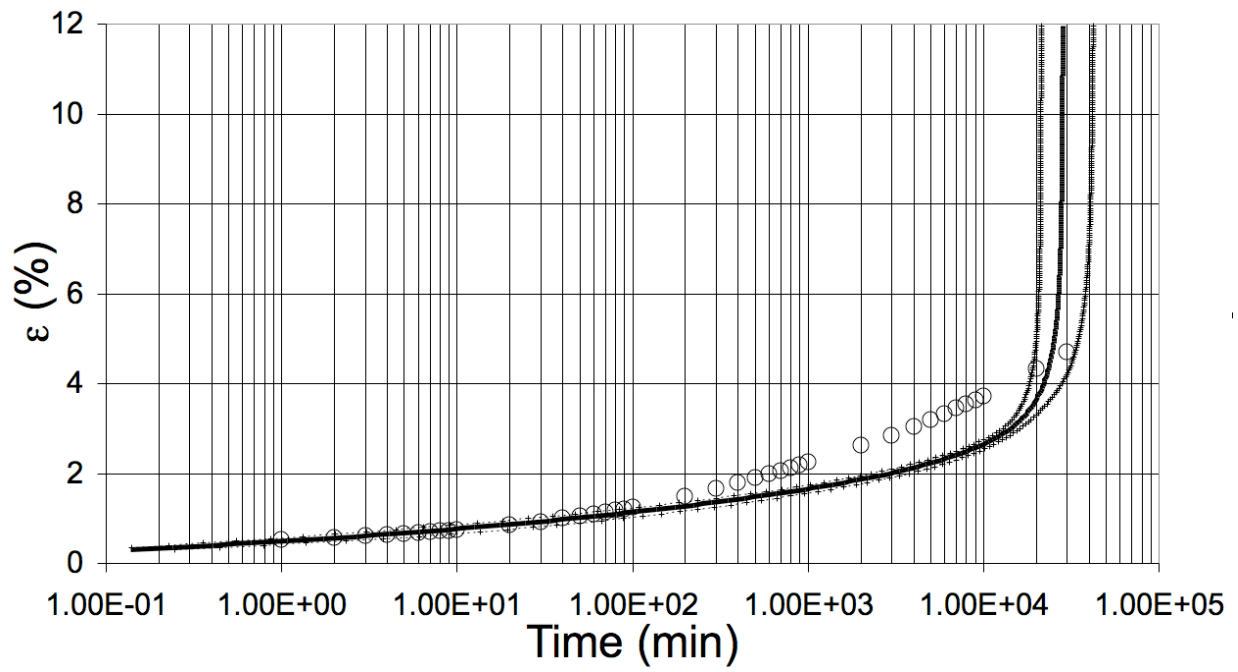
Figures 24 and 25 – Creep test - $\sigma_d/\sigma'_c = 0.552$



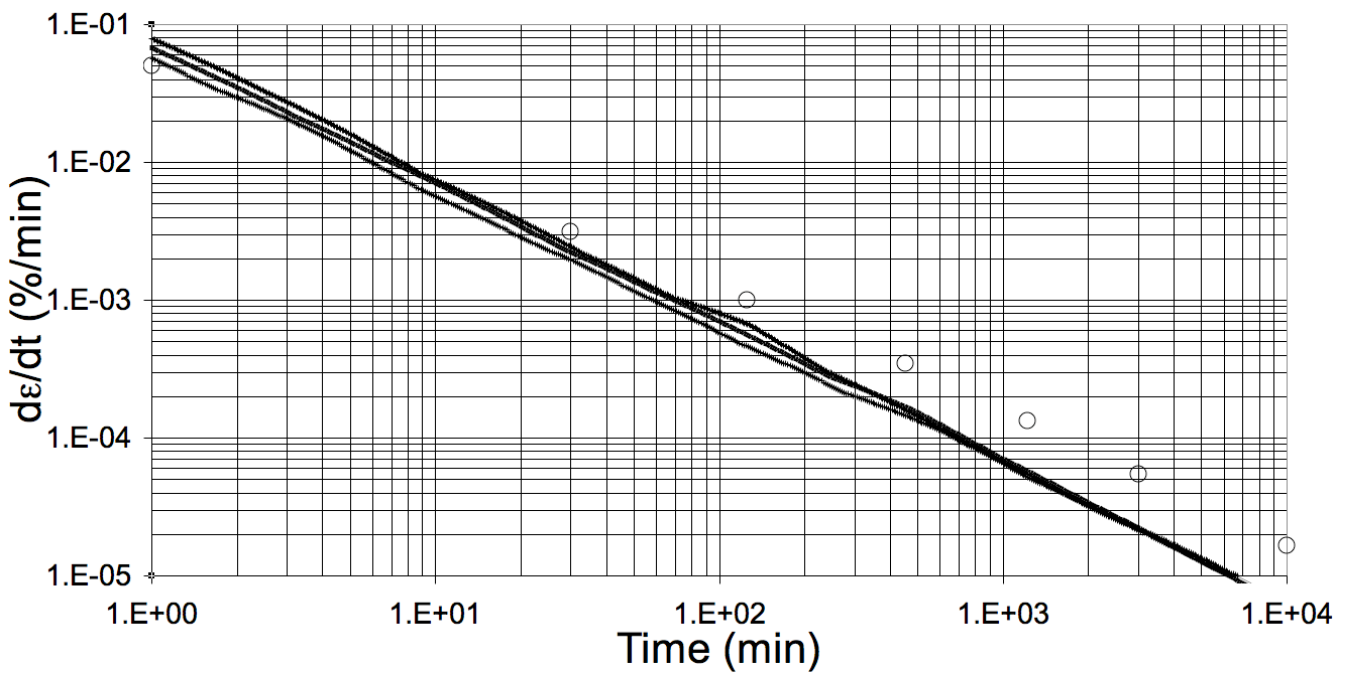
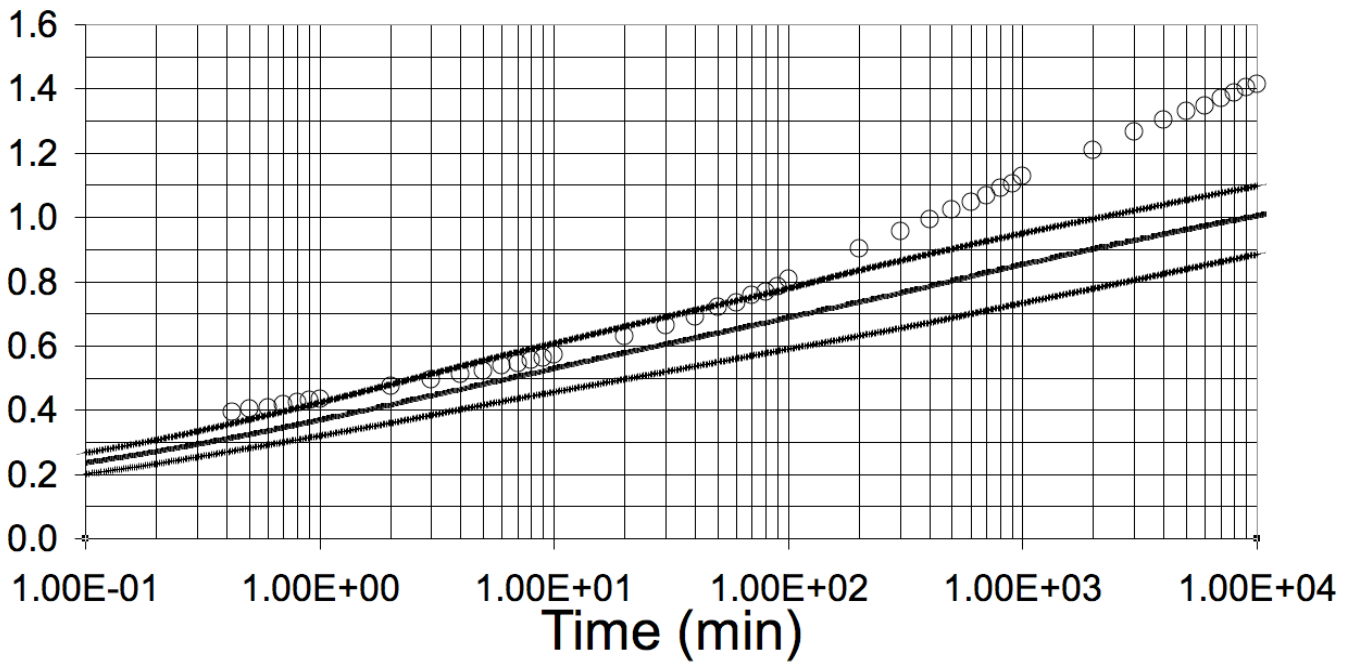
Figures 26 and 27 – Creep test - $\sigma_d/\sigma'_c = 0.530$



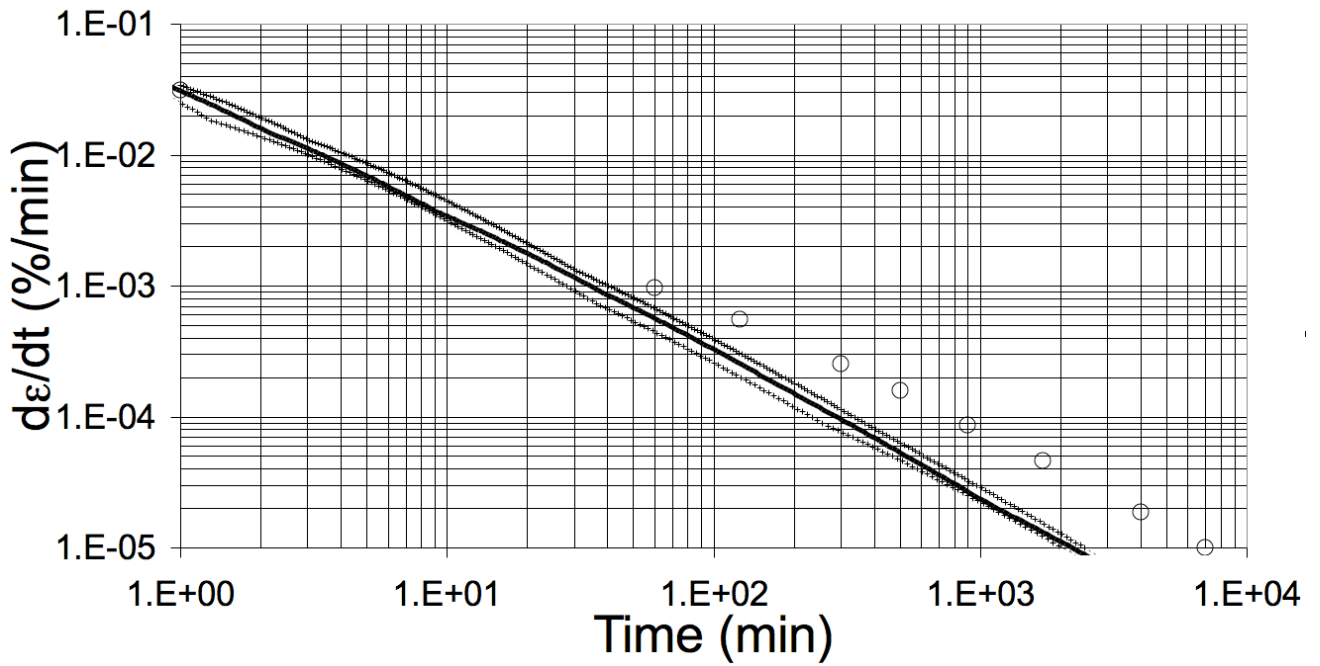
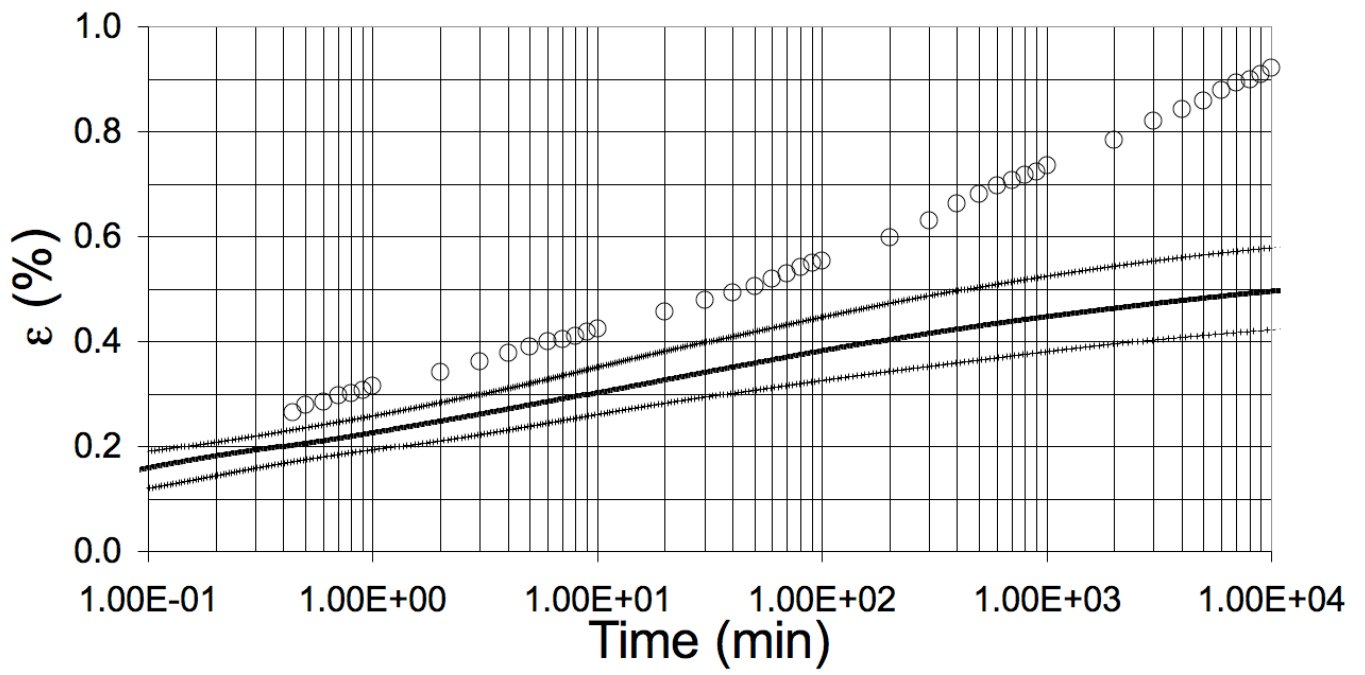
Figures 28 and 29 – Creep test - $\sigma_d/\sigma'_c = 0.518$



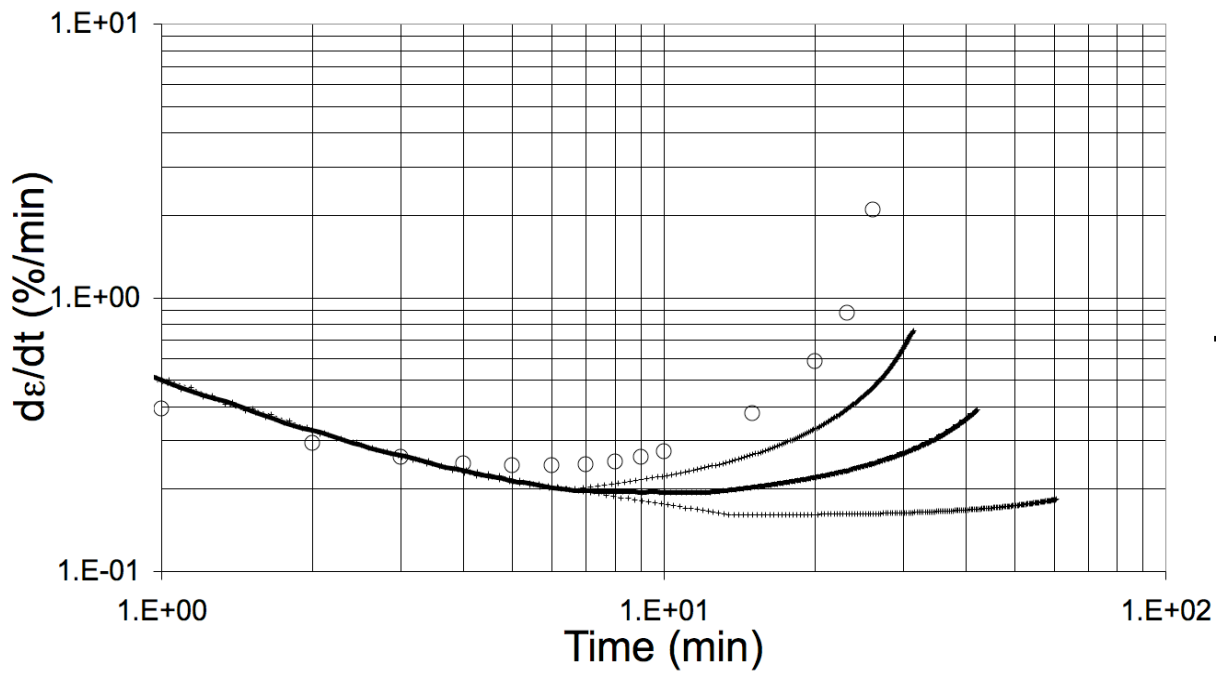
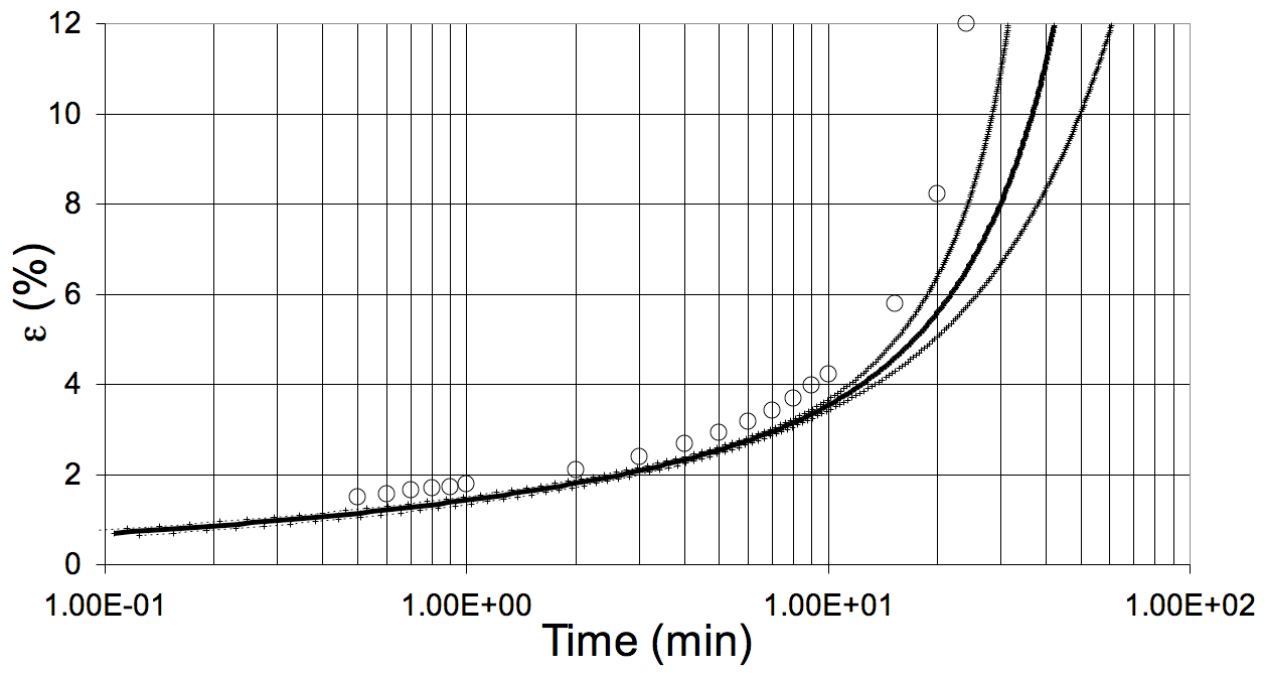
Figures 30 and 31 – Creep test - $\sigma_d/\sigma'_c = 0.500$



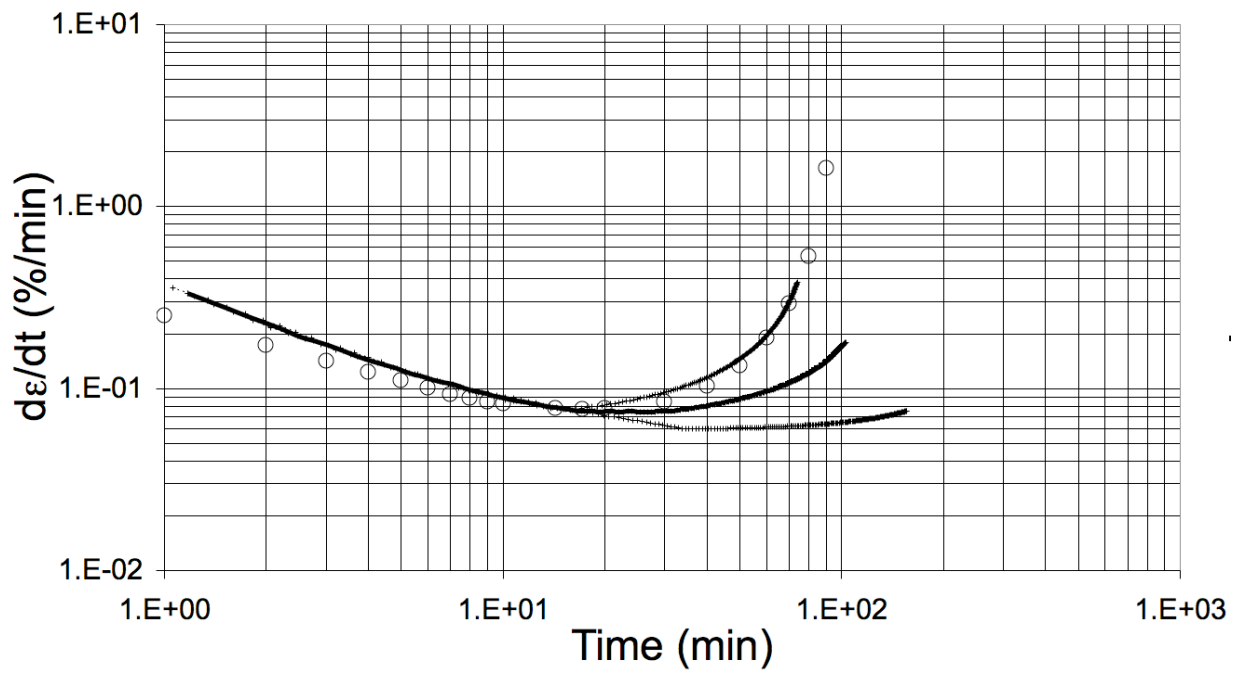
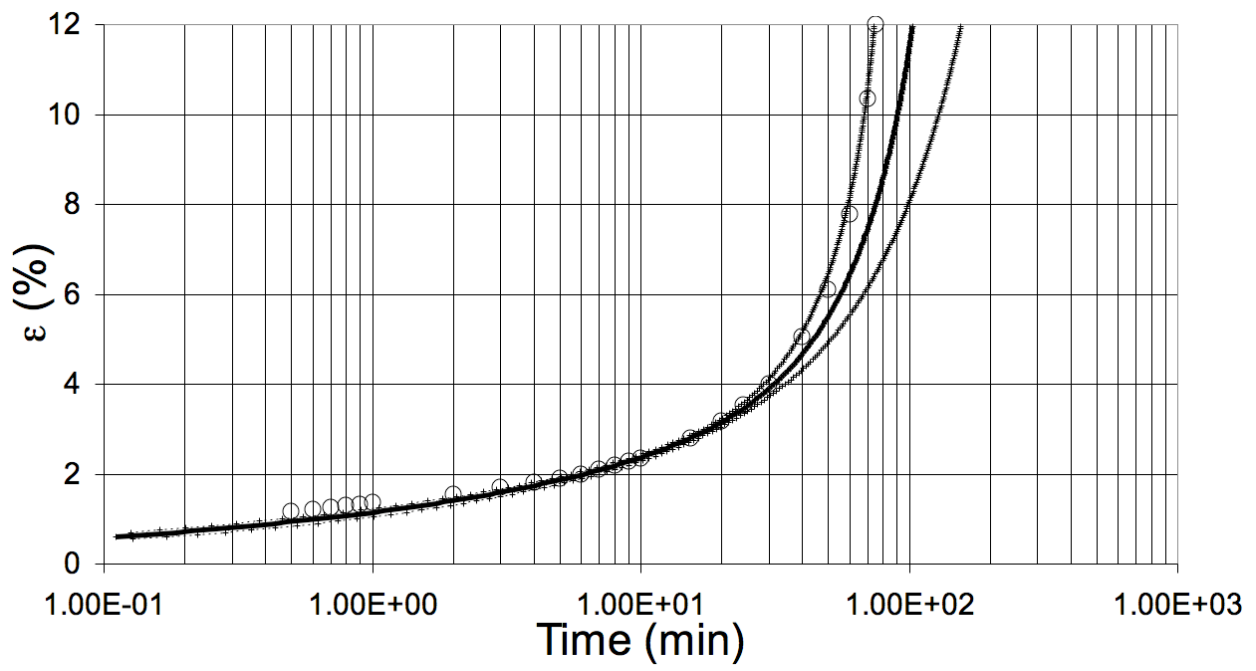
Figures 32 and 33 – Creep test - $\sigma_d/\sigma'_c = 0.446$



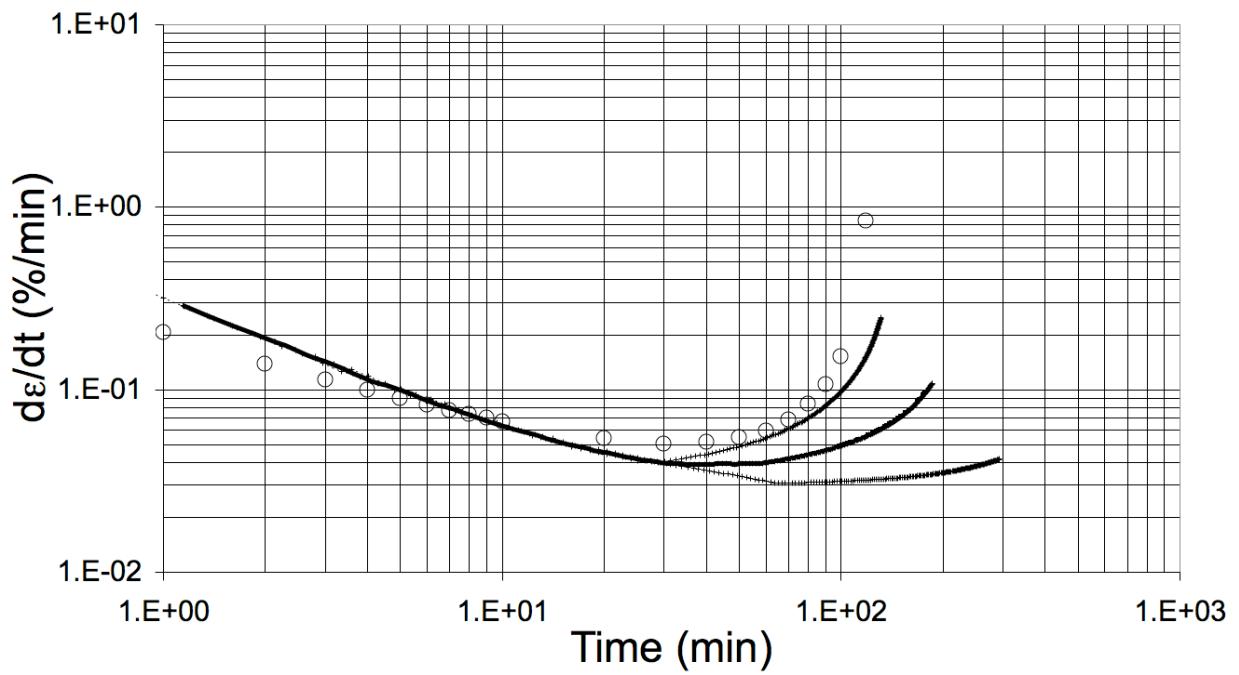
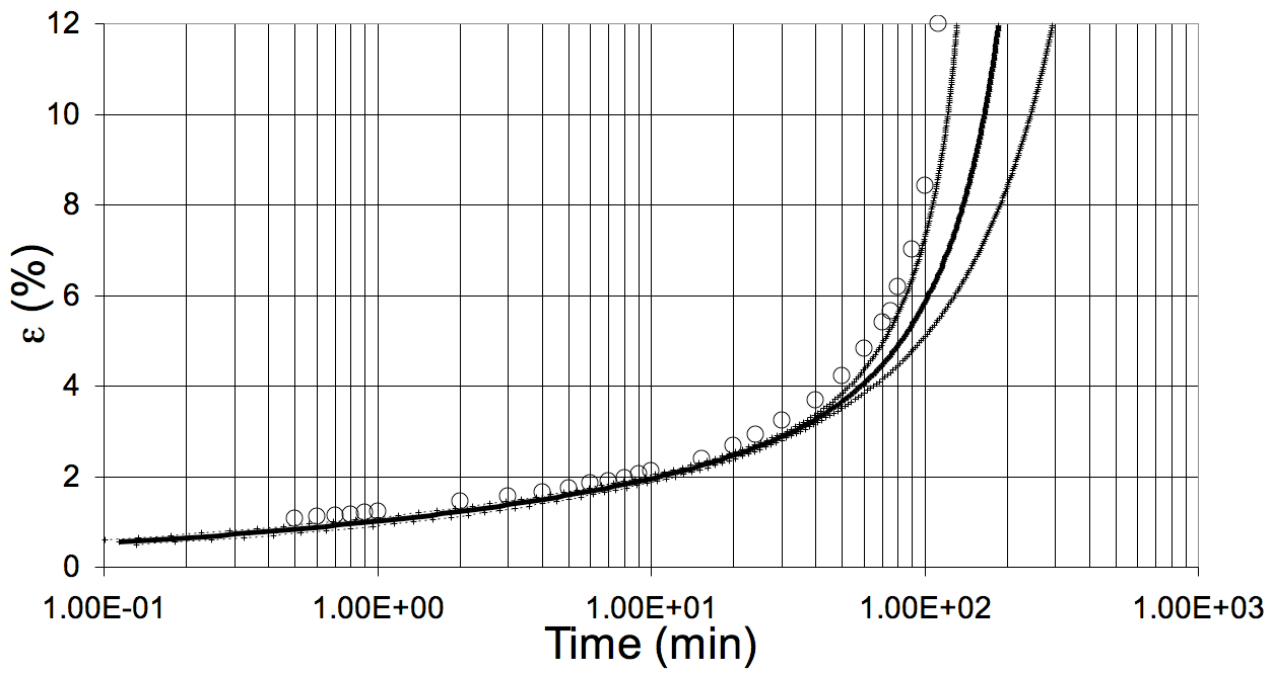
Figures 34 and 35 – Creep test - $\sigma_d/\sigma'_c = 0.374$



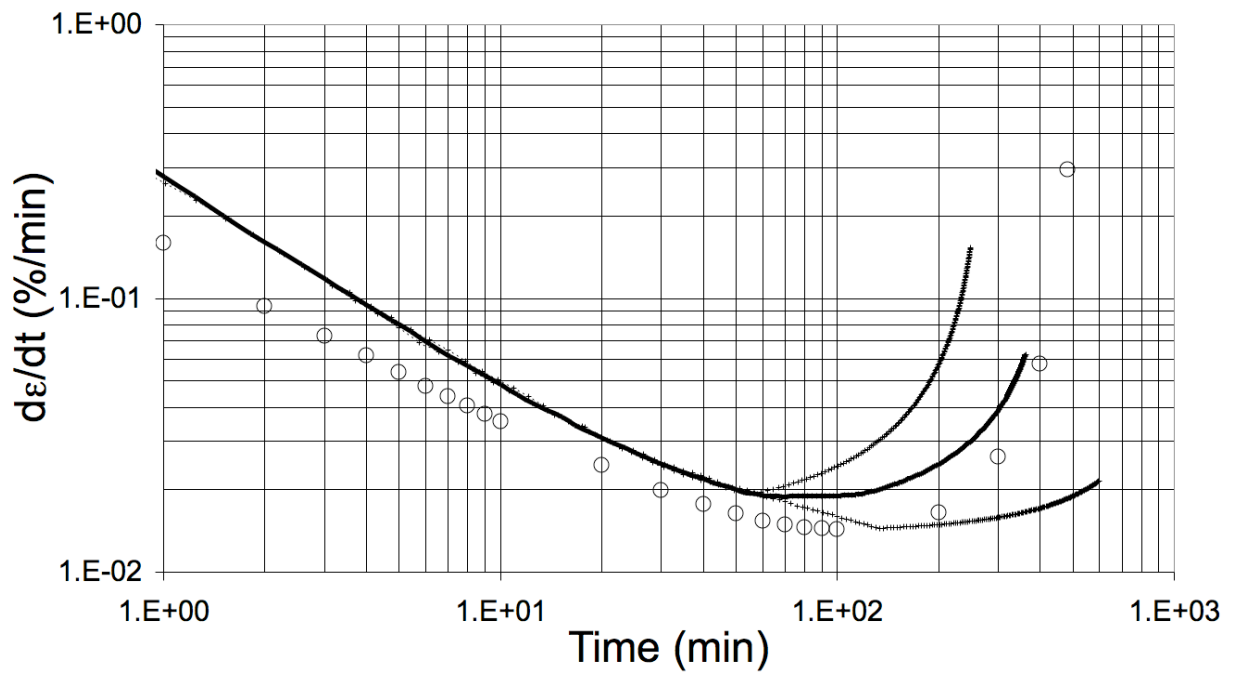
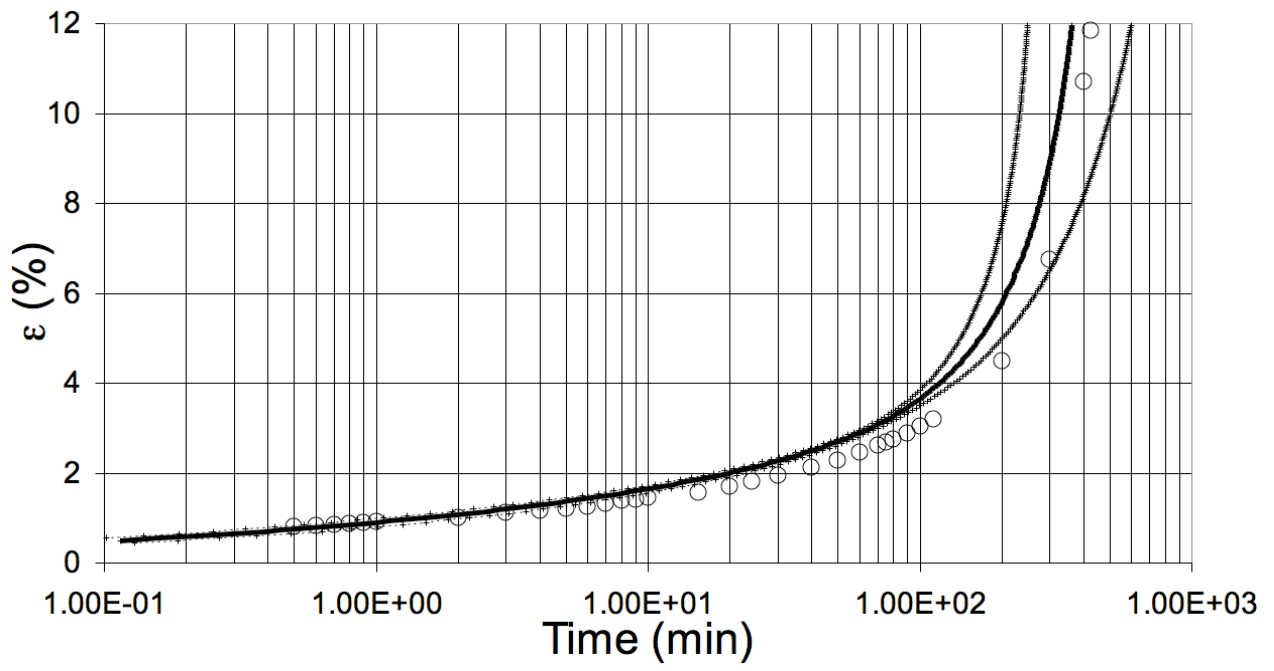
Figures 36 and 37 – Constant Load test - $\sigma_{d_0}/\sigma'_c = 0.630$



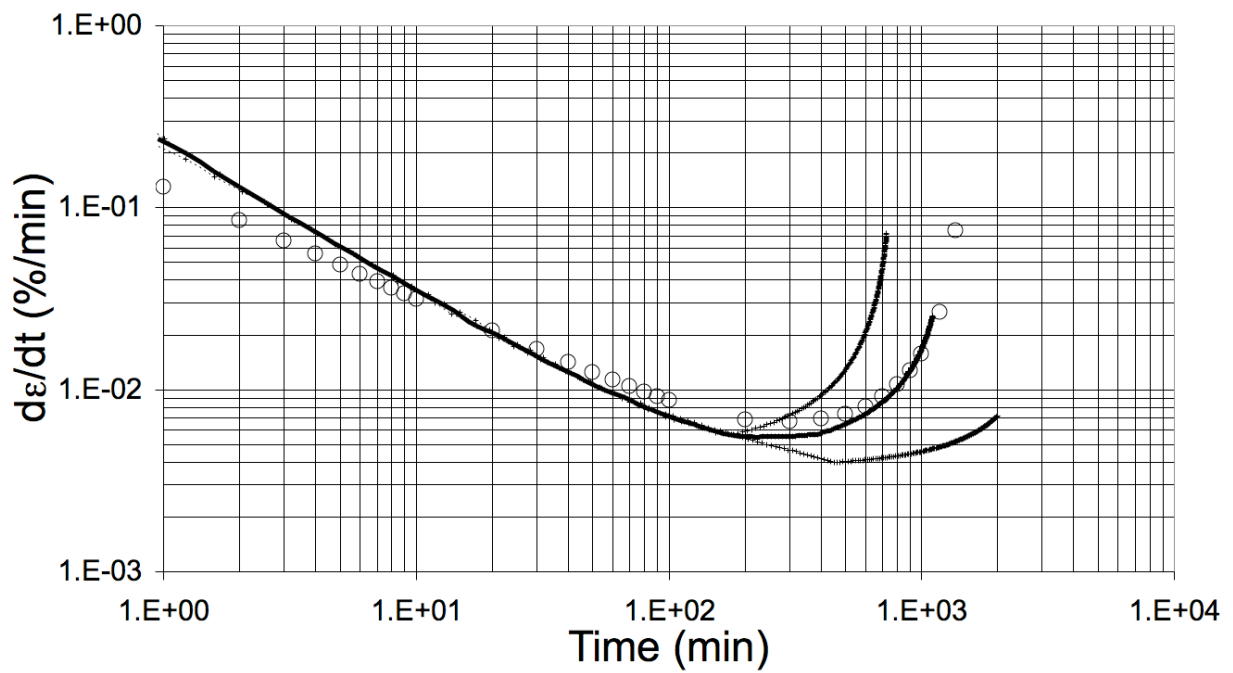
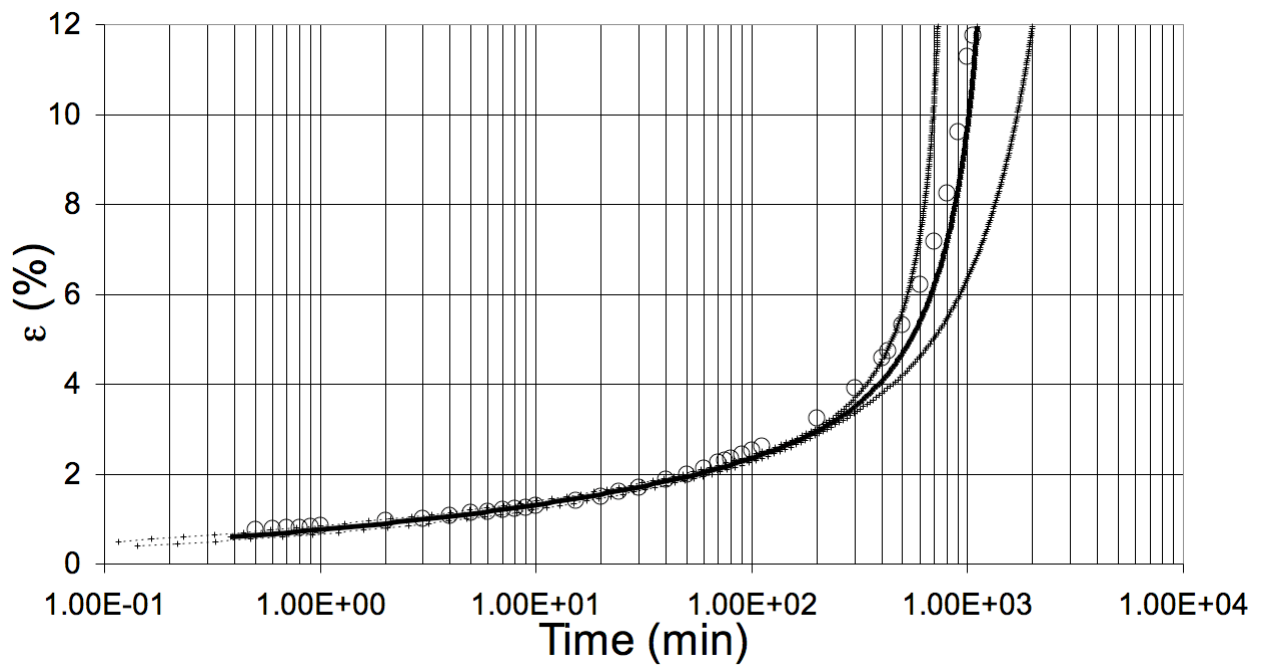
Figures 38 and 39 – Constant Load test - $\sigma_{d_0}/\sigma'_c = 0.606$



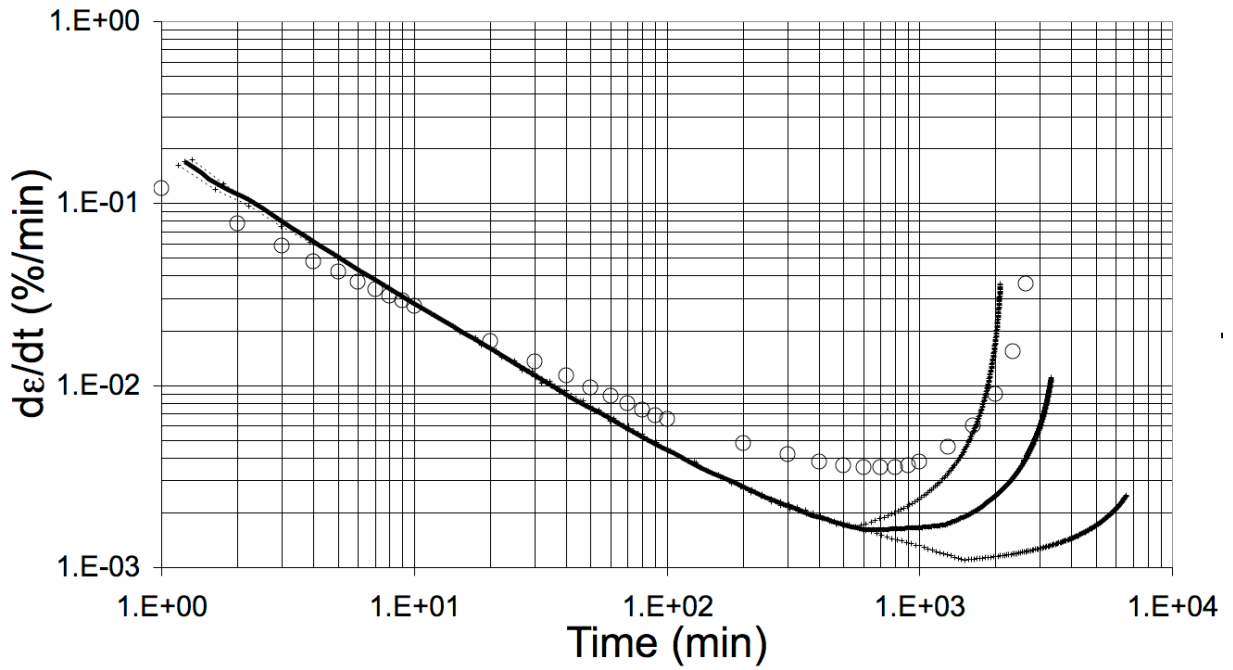
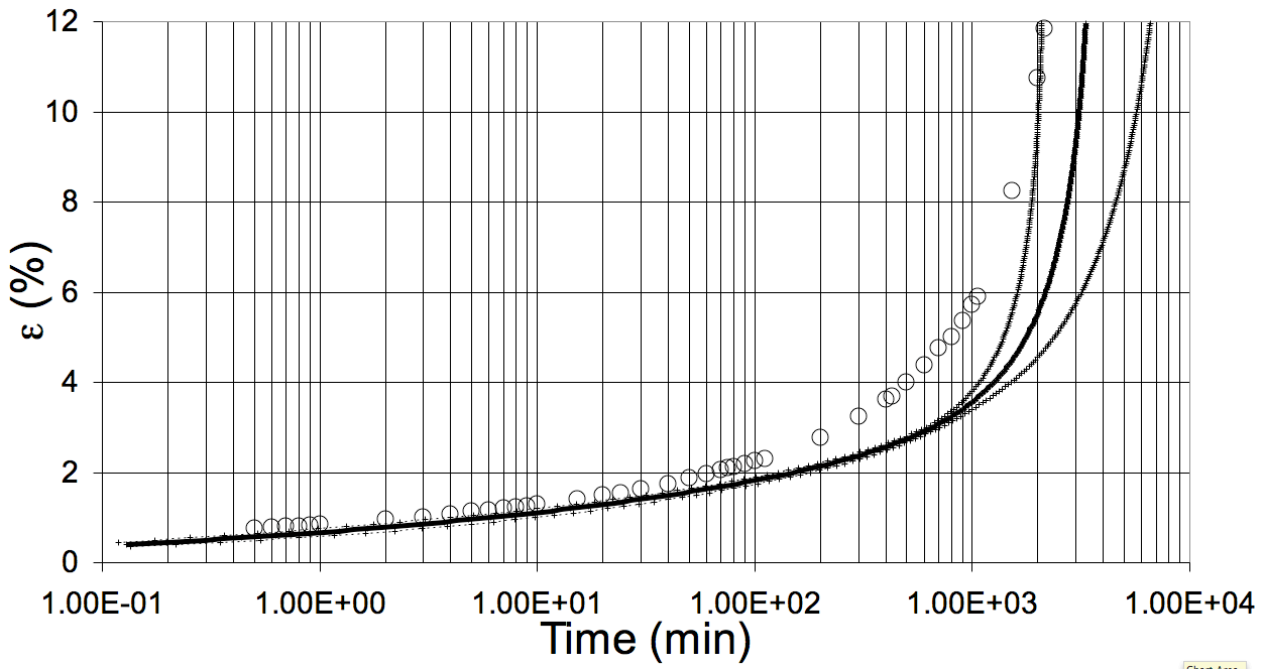
Figures 40 and 41 – Constant Load test - $\sigma_{d_0}/\sigma'_c = 0.592$



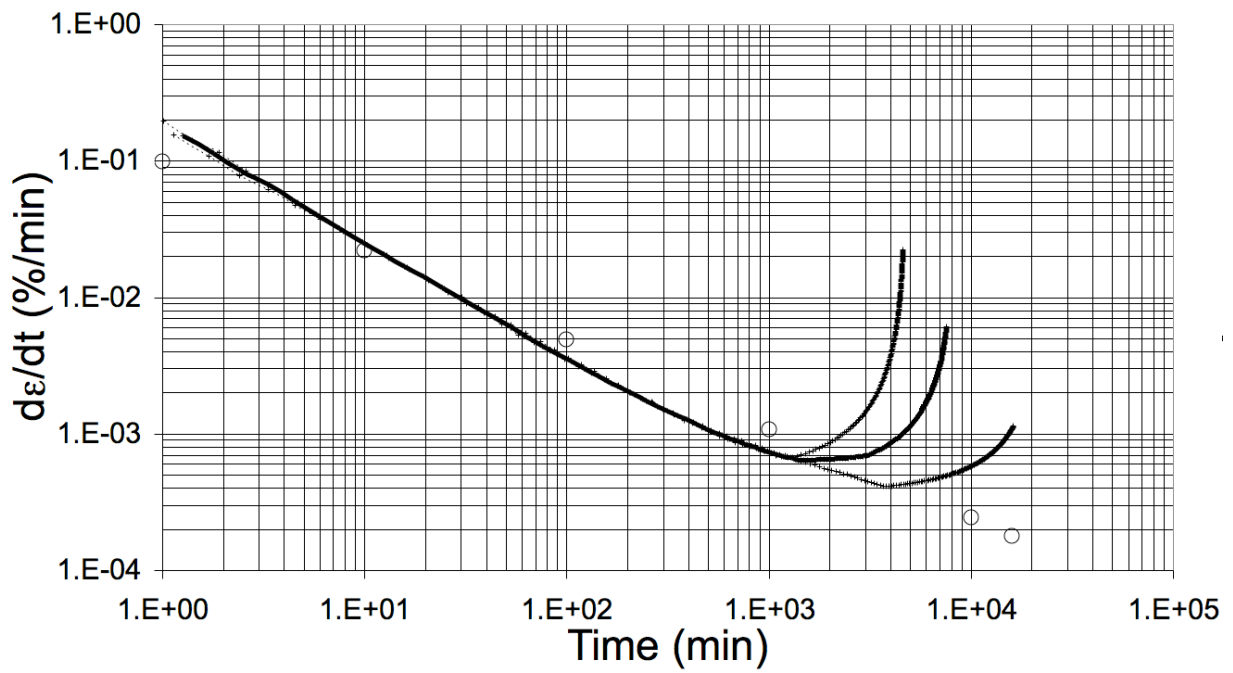
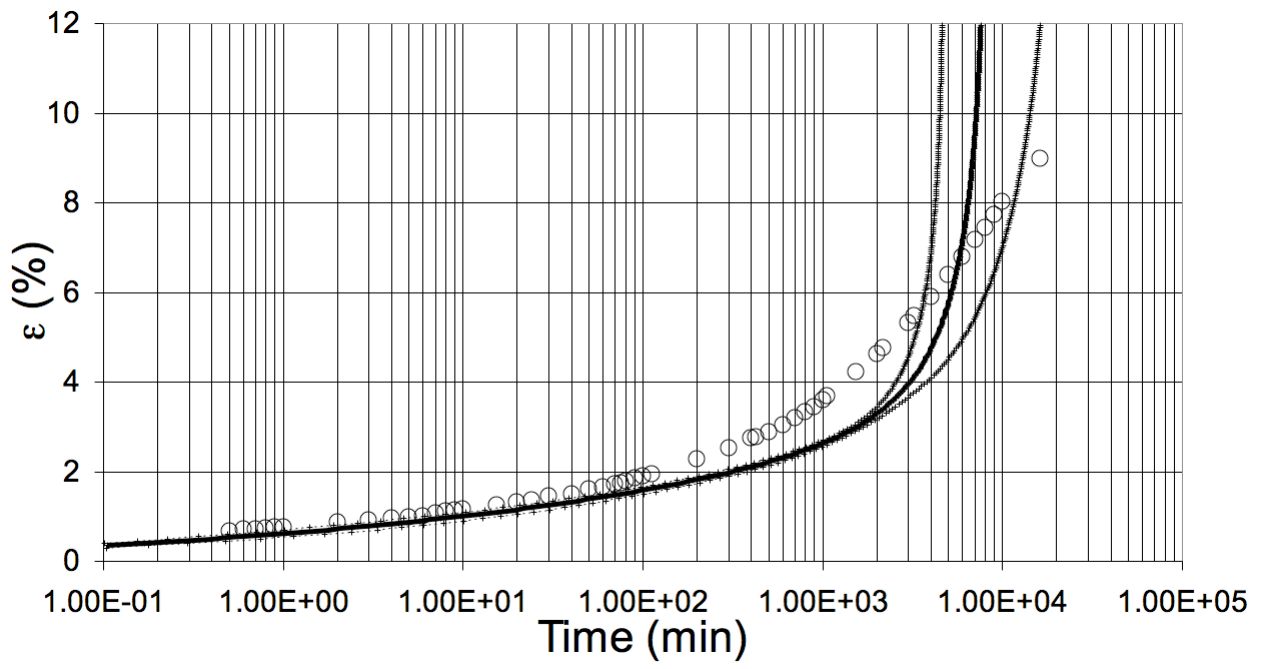
Figures 42 and 43 – Constant Load test - $\sigma_{d_0}/\sigma'_c = 0.578$



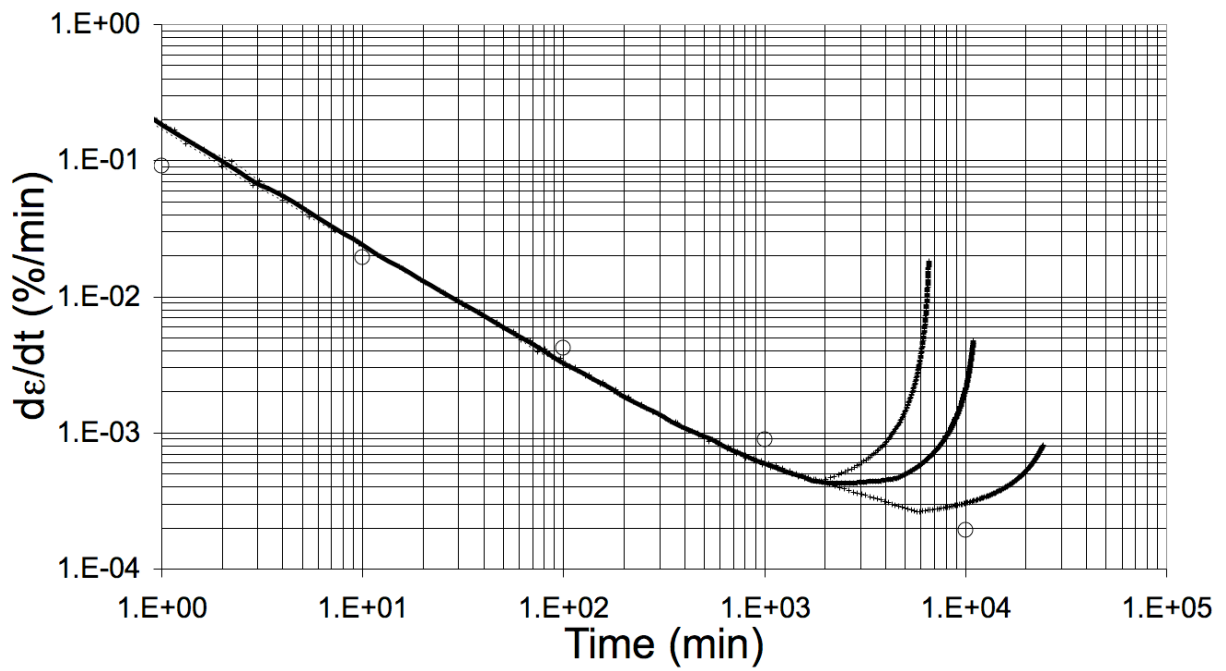
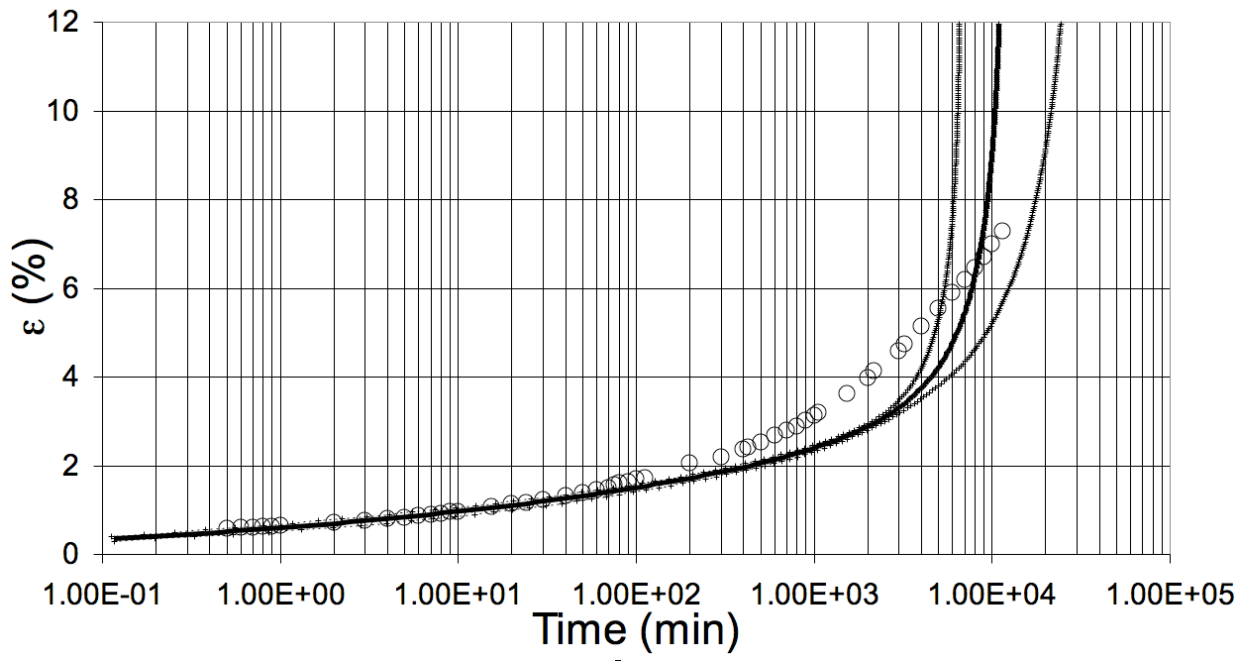
Figures 44 and 45 – Constant Load test - $\sigma_{d_0}/\sigma'_c = 0.558$



Figures 46 and 47 – Constant Load test - $\sigma_{d_0}/\sigma'_c = 0.542$



Figures 48 and 49 – Constant Load test - $\sigma_{d_0}/\sigma'_c = 0.532$



Figures 50 and 51 – Constant Load test - $\sigma_{d_0}/\sigma'_c = 0.528$

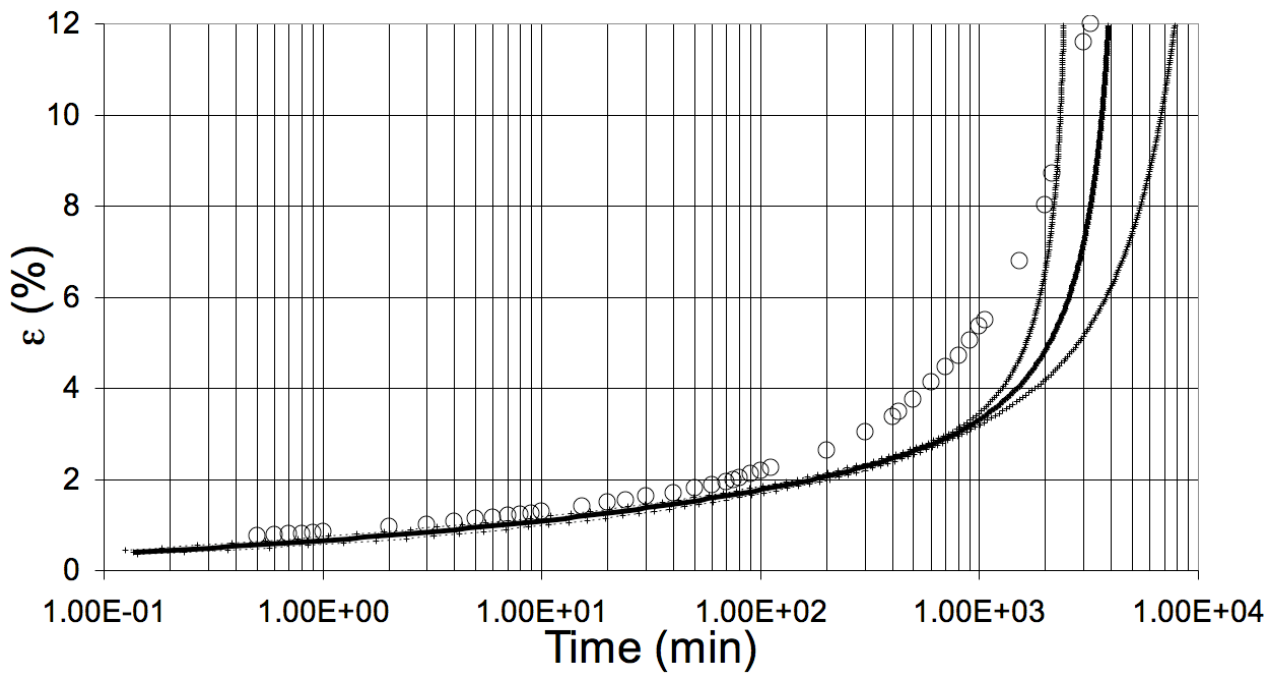


Figure 52 – Constant Load test - $\sigma_{d_0}/\sigma'_c = 0.540$

Discussion

Frictional and Viscous resistances

As attested by the correlation coefficient ($R^2 = 0.9988$), the power function represents the viscous resistance well for the range of strain rate of the laboratory tests. Also, the frictional resistances of all the laboratory tests, apart from some small variation, are very close to one another, supporting the hypotheses that the frictional resistance (for a given consolidation pressure and OCR) is an exclusive function of the shear strain and therefore independent of the strain rate.

Creep Tests

In general, it can be said that the numerical predictions carried out for the Creep Tests are satisfactorily, both qualitatively and quantitatively. However, a more detailed discussion will be presented below.

As mentioned in the Introduction, the three most important questions about creep behavior are:

- Will failure occur to a clay specimen subjected to a given stress state?
- If the specimen fails, how long will it take to fail? And;
- If not, what will be the final state of strain of the specimen and how long will it take for the specimen to reach it?

To answer the first question, it is sufficient to compare the applied deviatoric stress to the maximum frictional deviatoric stress. If the applied stress is greater than the maximum frictional resistance, the specimen will fail. On the other hand, if the applied stress is less than the maximum frictional resistance the specimen will not fail. Making this comparison for all the 11 laboratory tests, in accordance to the model, for creep tests with $\sigma_d/\sigma'_c = 0.638$, $\sigma_d/\sigma'_c = 0.616$, $\sigma_d/\sigma'_c = 0.600$, $\sigma_d/\sigma'_c = 0.586$, $\sigma_d/\sigma'_c = 0.572$, $\sigma_d/\sigma'_c = 0.552$, $\sigma_d/\sigma'_c = 0.530$, $\sigma_d/\sigma'_c = 0.518$ and $\sigma_d/\sigma'_c = 0.500$, failure was expected to occur and for creep tests with $\sigma_d/\sigma'_c = 0.446$ and $\sigma_d/\sigma'_c = 0.374$ failure

was not expected to occur. Therefore, except for test $\sigma_d/\sigma'_c = 0.500$, the numerical predictions are in agreement with the laboratory tests results.

The creep test with $\sigma_d/\sigma'_c = 0.500$ presents characteristics of failure and stabilization at the same time. This test appears to be stabilizing as the strain rate is continuously decreasing, but on the other hand, the strain after 32,000 min is about 4.6% and therefore above the peak strain which is about 2.5-3.0%. Taking into account these peculiar facts, the prediction made for this test is in agreement with the test results in the sense that strains greater than 2.5-3.0% were expected. Despite of this, the prediction is not in agreement with the test results as this test was expected to reach a minimum strain rate at about 10,000 to 15,000 minutes, which did not occur.

As Vaid and Campanella (1977) observed that thixotropic effects were observed after a time of about 20,000 minutes in creep tests with $\sigma_d/\sigma'_c = 0.446$ and $\sigma_d/\sigma'_c = 0.374$, perhaps the difference between the prediction and the test results for creep test with $\sigma_d/\sigma'_c = 0.500$ may be related to thixotropy as well.

Regarding the second question, the answers will be provided in the context of the definition of failure in a creep test according to Martins' model. According to the definition, failure will occur when $\dot{\epsilon} > 0$ and when $\ddot{\epsilon} \geq 0$. Therefore the onset of failure for a soil with a peak in strength is when the creep tests reach the minimum strain rate (which is consistent with the proposition made by Finn and Snead, 1973). For the Constant Rate of Strain tests, the peak is in the strain range of about 2.5 % to 3 % and therefore the minimum strain rates should occur within this range of strain. Table 4 below presents the predictions and the laboratory tests data:

Experimental Data				Predictions		
σ_d/σ'_c	Minimum $\dot{\epsilon}$ (%/min)	Time (min)	$\epsilon(\%)$	Minimum $\dot{\epsilon}$ (%/min)	Time (min)	$\epsilon(\%)$
0.638	0.24	4	2.45	0.483 – 0.481	2.9 – 3.6	2.5 – 3.0
0.616	0.12	9	2.38	0.224 – 0.227	5.9 – 7.4	2.5 – 3.0
0.600	0.054	20	2.57	0.119 – 0.121	10.6 – 13.5	2.5 – 3.0
0.586	0.04	23	2.25	0.065 – 0.066	18.9 – 24.2	2.5 – 3.0
0.572	2.7×10^{-2}	40	2.49	$3.25 \text{ a } 3.3 \times 10^{-2}$	35.9 – 46.5	2.5 – 3.0
0.552	6.9×10^{-3}	200	2.84	$1.0 \text{ a } 1.1 \times 10^{-2}$	105 – 133.7	2.5 – 3.0
0.530	2.0×10^{-3}	700	2.89	$2.0 \text{ a } 2.2 \times 10^{-3}$	467 - 610	2.5 – 3.0
0.518	3.3×10^{-4}	6000	4.92	$6.9 \text{ a } 7.1 \times 10^{-4}$	1307 - 1744	2.5 – 3.0

Table 4 – Comparison of minimum strain rate, time and strain for creep tests.

Finally, the third question can be answered by comparing the strains from the frictional resistance curve for the creep deviatoric stresses of tests $\sigma_d/\sigma'_c = 0.446$ and $\sigma_d/\sigma'_c = 0.374$ with the strains of these tests. The predictions for test $\sigma_d/\sigma'_c = 0.446$ and $\sigma_d/\sigma'_c = 0.374$ are between $\epsilon = 1.4\%$ and $\epsilon = 1.6\%$, and for test $\sigma_d/\sigma'_c = 0.374$ are between $\epsilon = 0.5\%$ and $\epsilon = 0.7\%$. The experimental results for tests $\sigma_d/\sigma'_c = 0.446$ and $\sigma_d/\sigma'_c = 0.374$, when they were roughly terminated between about 2 and 3 weeks, are respectively $\epsilon = 1.5\%$ and $\epsilon = 1.0\%$.

Regarding the time for stabilization, the comparison between prediction and test results are not possible as, according to Equation (7), the behavior is asymptotic. However, it is possible to compare the values of the strain rates for the last experimental data point. For this data point, the strain rate for tests $\sigma_d/\sigma'_c = 0.446$ and $\sigma_d/\sigma'_c = 0.374$ at $t = 10,000$ min and $t = 7,000$ min are 1.55×10^{-5} %/min and 1×10^{-5} %/min, respectively. According to the predictions, the strain rates range from 1.14 to 1.55×10^{-5} %/min for test with $\sigma_d/\sigma'_c = 0.446$ and from 1.3 to 1.6×10^{-5} %/min for test

with $\sigma_d/\sigma'_c = 0.374$.

In relation to the variation of the strain rate with time, Figure (7), it can be seen that the curves for tests $\sigma_d/\sigma'_c = 0.446$ and $\sigma_d/\sigma'_c = 0.374$, when represented in a $\log (de/dt) \times \log (t)$ plot, are not perfectly straight but slightly curved downwards.

The examination of Equation (8) allows for an interpretation of the shape of this curve. Equation (8) was obtained considering that the relationship between frictional deviatoric stresses and strains can be represented by a straight line. However, the stress-strain diagram of a real soil is not straight. Considering that Equation (8) can be applied by parts, in intervals in which E can be assumed constant, for each interval a different Equation (8) with its respective E modulus can be applied. The effect of the modulus E on Equation (8) is such that, having all the other parameters the same, the curve is displaced to the right for decreasing values of the E modulus. The Figure below exemplifies this point.

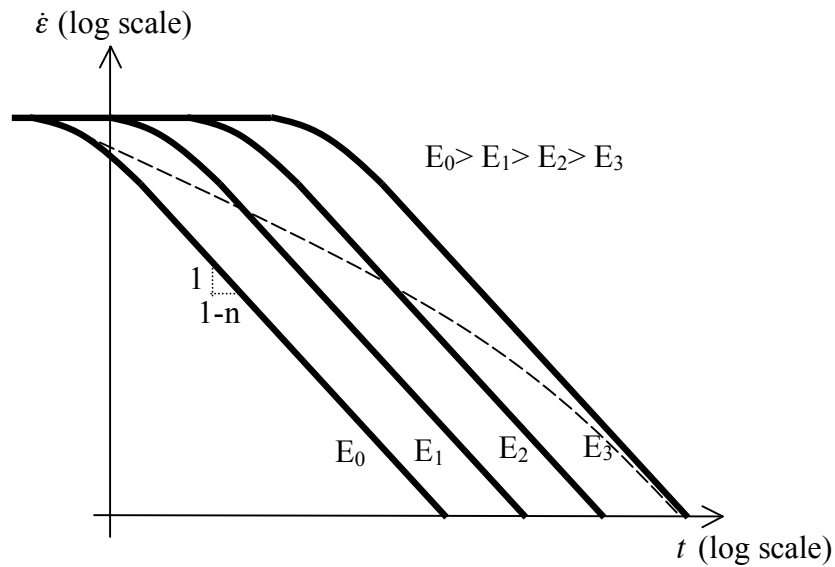


Figure 53 – Effect of E on Equation (8).

Now consider a frictional deviatoric stress curve such as the one represented in the Figure below and an undrained creep test with a deviatoric stress σ_{d_3} .

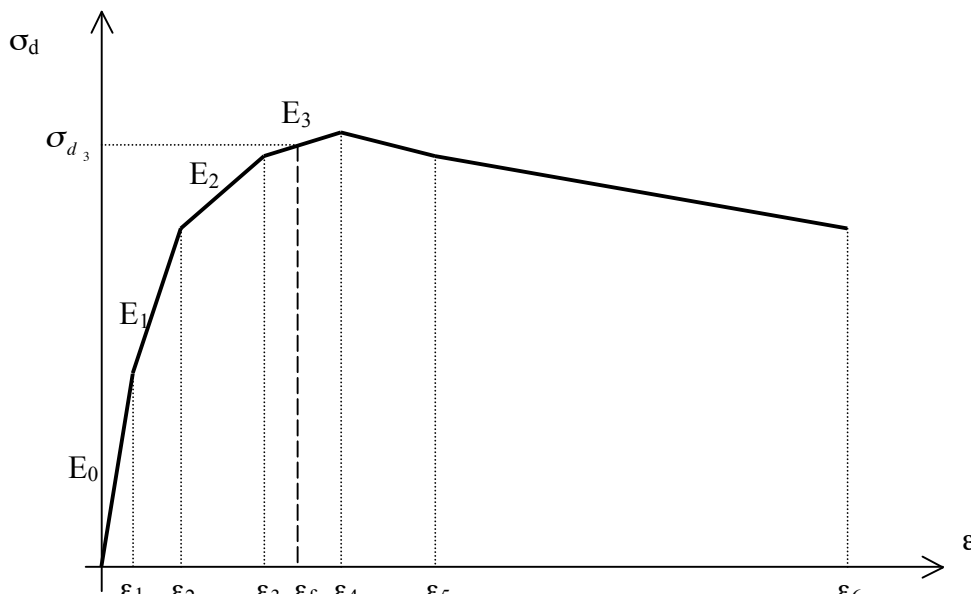


Figure 54 – Discretization of a frictional deviatoric stress curve with constant E by parts.

According to the concepts developed so far, it is expected that this creep test will stabilize at a strain $\varepsilon = \varepsilon_f$ where the modulus is E_3 . However, before reaching this strain, the specimen will reach strains between $\varepsilon = \varepsilon_3$ and $\varepsilon = \varepsilon_2$, where the modulus is E_2 , and before that, strains between $\varepsilon = \varepsilon_2$ and $\varepsilon = \varepsilon_1$ where the modulus is E_1 . Therefore, the strain rate x time curve of this specimen will start at a curve representing Equation (8) where the modulus is E_0 , for $\varepsilon = 0$, cross the curves relative to E_1 and E_2 and reach (asymptotically) the curve where the modulus is E_3 . In the process of crossing these curves and reaching the curve relative to E_3 , the curve of the specimen subjected to the creep stress presents itself slightly convex. This effect is expected to be more pronounced for creep tests with higher applied deviatoric stresses (that do not fail) and for soils presenting strongly curved stress-strain curves before reaching its maximum strength value.

For assessing these “boundary lines”, the following equation can be used:

$$\dot{\varepsilon} = \frac{1}{\left[\left(\frac{K/\sigma'_c}{\sigma_d/\sigma'_c} \right)^{\left(\frac{1-n}{n} \right)} + \left(\frac{1-n}{n} \right) \cdot \frac{(E/\sigma'_c) \cdot t}{(K/\sigma'_c)} \right]^{\left(\frac{1}{1-n} \right)}} \quad (16)$$

Equation (16) is Equation (8) normalized in relation to σ'_c .

Regarding the creep test with $\sigma_d/\sigma'_c = 0.446$, from Figure 12, for $\varepsilon = 1.55\%$ and $\varepsilon = 0\%$, E/σ'_c modulus of about $E/\sigma'_c = 0.033\%^{-1}$ and $E/\sigma'_c = 1.65\%^{-1}$ can be assessed respectively. For creep test with $\sigma_d/\sigma'_c = 0.374$, from Figure 12, for $\varepsilon = 1.0\%$ and $\varepsilon = 0\%$, E/σ'_c modulus of about $E/\sigma'_c = 0.084\%^{-1}$ and $E/\sigma'_c = 1.65\%^{-1}$ can be assessed respectively.

For these values and considering that $K/\sigma'_c = 0.200 \text{ min}^{0.174}$ and that $n = 0.174$, the strain rate for a given time can be assessed using Equation (16) and the parameters mentioned above, the following strain rates were assessed for the selected times shown in the table.

σ_d/σ'_c	$\varepsilon(\%)$	$E/\sigma'_c (\%^{-1})$	Time (min)	$\dot{\varepsilon} (\%/min)$
0.446	1.55	0.033	10	8.2×10^{-2}
			100	5.1×10^{-3}
			1000	3.1×10^{-4}
	0	1.65	1	1.2×10^{-2}
			10	7.3×10^{-4}
			100	4.5×10^{-5}
0.374	1.0	0.084	10	2.7×10^{-2}
			100	1.6×10^{-3}
			1000	1.0×10^{-4}
	0	1.65	1	1.2×10^{-2}
			10	7.3×10^{-4}
			100	4.5×10^{-5}

Table 5 – Assessment of the “boundary” lines for creep tests with $\sigma_d/\sigma'_c = 0.446$ and $\sigma_d/\sigma'_c = 0.374$.

The “boundary” lines assessed on Table 5 are shown as thick dashed lines in the figures below:

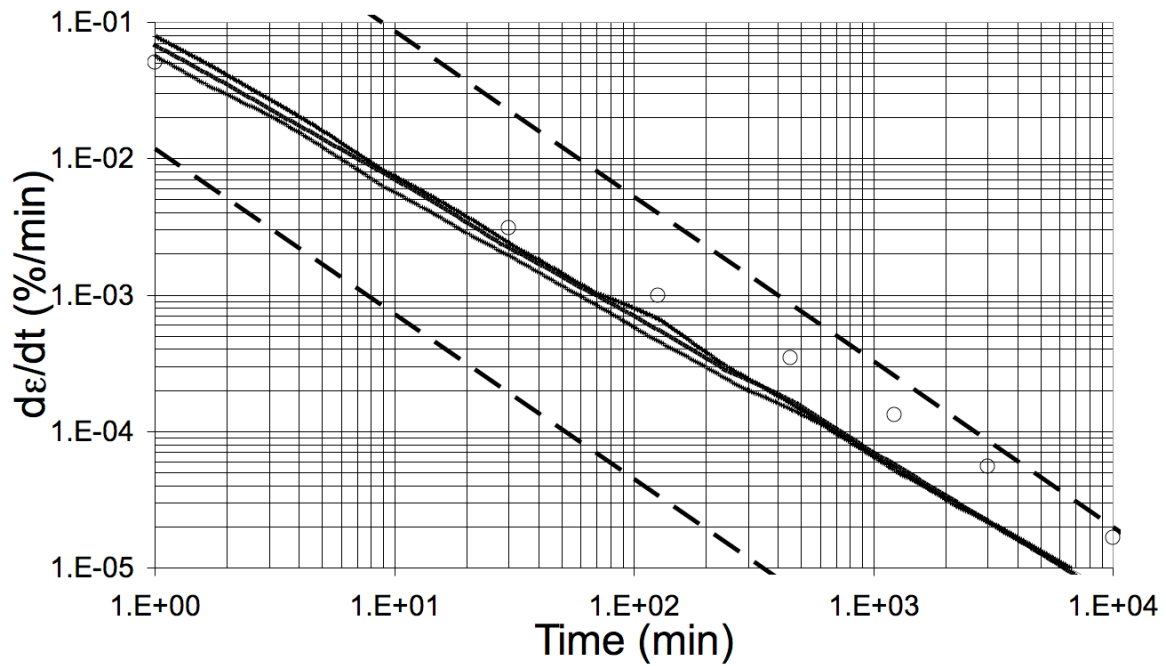


Figure 55 – Strain rate x time boundary lines for test with $\sigma_d/\sigma'_c = 0.446$.

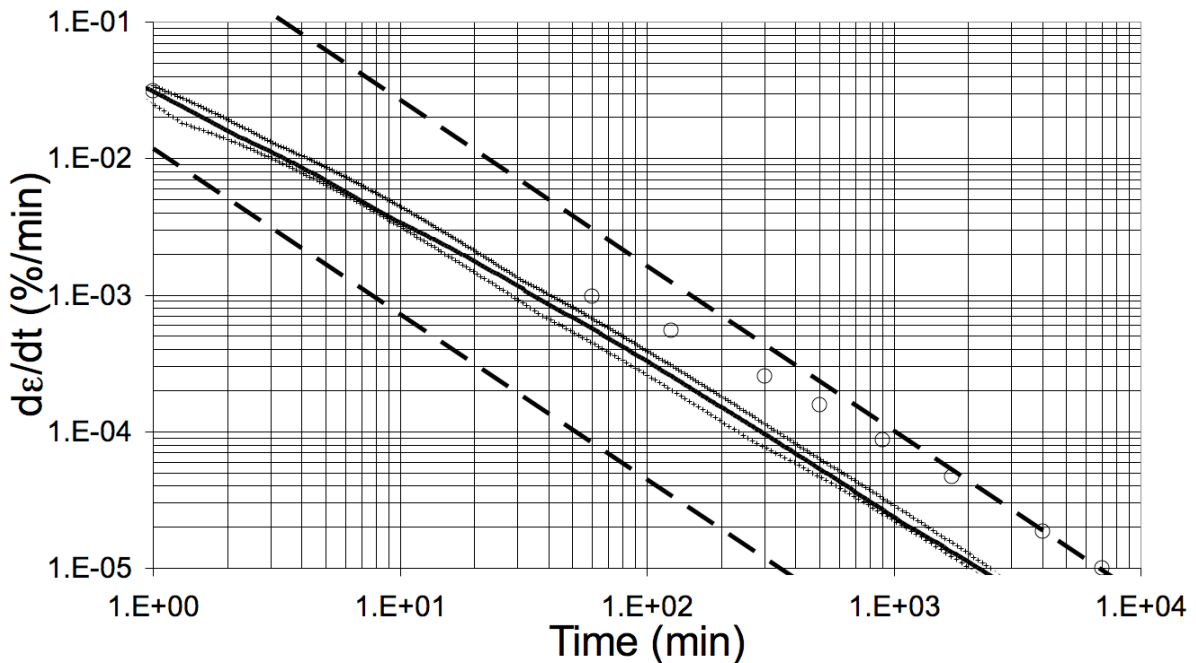


Figure 56 – Strain rate x time boundary lines for test with $\sigma_d/\sigma'_c = 0.374$.

In addition, the convexity of the strain rate x time curve can, of course, be seen on Figure 7 as well.

When all the test results are compared together it can be seen that, in general, for creep tests with a deviatoric stress equal or smaller than $\sigma_d/\sigma'_c = 0.518$ the prediction deviate more from the tests results than the other tests. Looking at the strain rate, it appears that tests that presented strain rates below 1×10^{-3} %/min show greater deviations than the others. The effect of the strain rate can also be seen on the Constant Rate of Strain tests. The tests with constant strain rate equal or lower than 2.8×10^{-3} %/min show a smaller decrease in the strength with strain than the others. Therefore it is believed that $\sigma_d/\sigma'_c = 0.518$ was affected by the thixotropy.

Constant Load Tests

In general, it can be said that the predictions carried out for the Constant Load Tests are also satisfactory, both in qualitative and quantitative terms. As for the Creep tests results, a more detailed discussion will be presented below for the Constant Load tests.

As the load is constant and the cross section area of the specimen increases with strain, the initial deviatoric stress decreases with strain as well. As pointed out before, the current deviatoric stress is related to the initial deviatoric stress by the equation $\sigma_d = \sigma_{d_0} \cdot (1 - \epsilon)$. In this context, to answer the first question about the failure of a specimen subject to a given deviatoric stress, it is necessary to compare the current deviatoric stress with the frictional deviatoric stress for the same strain. This comparison can be made with the help of Figure 57 below.

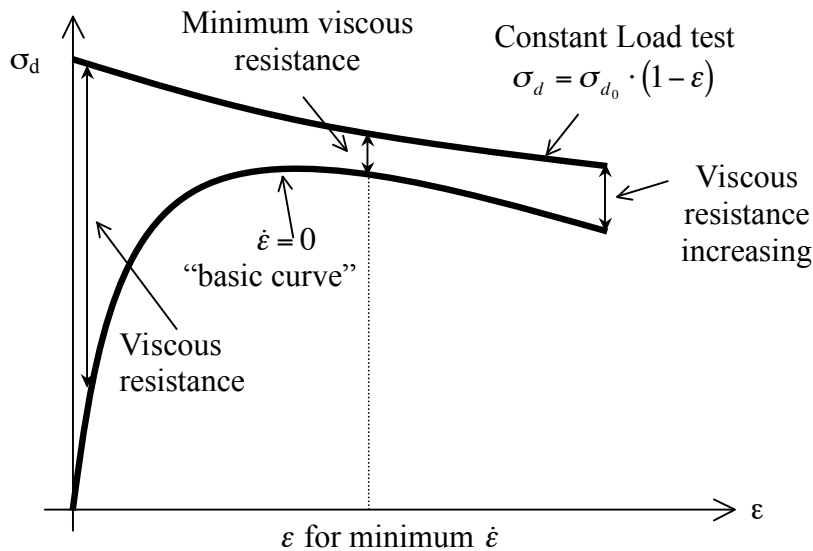


Figure 57 - Constant Load Test.

If the current frictional deviatoric stress is greater than the frictional deviatoric stress (for the same strain), the specimen will continue to deform. That means, if the constant load test curve is above the frictional deviatoric curve for any strain, the specimen will not stabilize. Stabilization will occur only if the current stress curve “touches” the frictional resistance curve.

Undertaking this comparison for the Constant Load Tests, it is predicted that no test will stabilize for the range of strains experienced by the tests. The tests results show that in fact 7 of the 9 tests fail by reaching the minimum strain rate and presenting an increase in the strain rates afterwards. Tests $\sigma_{d_0}/\sigma'_c = 0.532$ and $\sigma_{d_0}/\sigma'_c = 0.528$ did not pass through a minimum in strain rate although they experienced large strains (greater than about 7% in both tests) as predicted. In accordance to the concept that, by having a constant load curve above the frictional curve the specimen will not stabilize, these two tests can also be considered to have failed. Therefore predictions and test results regarding stabilization agree.

The question about the minimum strain rate and its relationship with the strains will be addressed considering the stress decrease with the development of strains that occurs in a Constant Load Test.

Because of the shape of the current deviatoric stress function, the minimum viscous resistance, and therefore, the minimum strain rate, will not necessarily occur for the strain related to the peak strength, but for a strain somewhat greater than that. The minimum strain rate will occur for the

strain where the viscous resistance is minimum. For the values of the initial deviatoric stresses of the tests carried out by Vaid and Campanella (1977) and considering the shape of the frictional resistance, the strain interval within which the minimum strain rates are expected to occur are between 2.9% and 4%. Table 6 below presents the predictions and the tests results data.

Experimental Data				Predictions		
σ_{d0}/σ'_c	Minimum $d\varepsilon/dt$ (%/min)	Time (min)	ε (%)	Minimum $d\varepsilon/dt$ (%/min)	Time (min)	ε (%)
0.630	0.243	6	3.17	0.161 to 0.2	6.4 to 13.8	2.7 to 4.0
0.606	7.7×10^{-2}	17.2	2.80	6.0 to 7.6×10^{-2}	15.8 to 34.6	2.9 to 4.0
0.592	5.1×10^{-2}	30	3.23	3.1 to 4.0×10^{-2}	28.9 to 65.2	2.9 to 4.0
0.578	1.4×10^{-2}	100	3.05	1.4 to 1.9×10^{-2}	57 to 133.2	2.9 to 4.0
0.558	6.7×10^{-3}	300	3.91	4.9 to 6.7×10^{-3}	179.2 to 449.5	2.9 to 4.0
0.542	3.6×10^{-3}	700	4.77	1.1 to 1.7×10^{-3}	556 to 1510	2.9 to 4.0
0.532	No minimum strain rate reached			4.1 to 6.7×10^{-4}	1277 to 3906	2.9 to 4.0
0.528	No minimum strain rate reached			2.65 to 4.44×10^{-4}	1868 to 5925	2.9 to 4.0

Table 6 – Comparison between predictions and the Constant Load tests results for the point of minimum strain rate.

Comparison with test $\sigma_{d0}/\sigma'_c = 0.540$ was not possible as the strain rate vs time curve of this test was not presented by Vaid and Campanella (1977).

Apart from this test for which a comparison was not possible, it can be seen agreement between predictions and test results in 6 of the 8 tests.

It is believed that the difference between the predictions and the tests results for Constant Load tests with $\sigma_{d0}/\sigma'_c = 0.532$ and $\sigma_{d0}/\sigma'_c = 0.528$ may also be attributed to the thixotropy effects as these were the only Constant Load tests that presented strain rates below 1×10^{-3} %/min.

Conclusions

Considering the results of the predictions for the sensitive undisturbed Haney Clay, the following conclusions can be made:

- The separation of the shear strength of the Haney Clay into the frictional and viscous resistances for explaining the undrained creep behavior of the Haney Clay, as established by Martins (19992), can be considered adequate;
- The viscous resistance can be represented by a power law function of the strain rate for the range of strain rates observed in this study;
- The hypothesis of considering the frictional resistance as a unique function of the shear strain, and therefore independent of the strain rate, as established by Martins, was verified for the Haney Clay;
- The hypothesis of normalization, as adopted by Martins (1992) was also verified for the Haney Clay;
- The undrained behavior under constant stress or constant load for the Haney Clay can be considered as a unique process, an interaction between frictional and viscous resistances, and not a segmented one.
- The minimum strain rates in creep tests are associated with the peak strength strain range as the minimum viscous resistance occurs within this strain range.
- The minimum strain rates for the constant load tests occur at strains greater than the peak strength strain. However, the minimum strain rates for these tests are also associated with

- the minimum viscous resistance which occur for a different strain range than the creep tests.
- The so-called “tertiary” creep, for the Haney Clay, can be considered as a consequence of the decrease of the frictional resistance and therefore increase in the viscous resistance of the soil;
- The model developed by Martins (1992) for non-sensitive, saturated, normally consolidated clays, as modified by Alexandre (2006), was able to predict qualitatively the behavior of the sensitive Haney Clay. The model was also able to predict quantitatively the behavior of the Haney Clay for the tests not affected by the thixotropy.

Acknowledgements

The authors wish to thank Professor Yoginder Vaid, Professor Emeritus of the University of British Columbia for the discussions and criticism and Mrs. Mei Cheung, M.Sc., P. Eng., for the reading of this manuscript, discussions and for the many suggestions presented.

References

Adachi T., Okano M., (1974), A constitutive equation for normally consolidated clay, *Soils and Foundations*, 14, (4), 55-73.

Alexandre (2006), Contribution to the Understanding of the Undrained Creep, D.Sc. thesis, COPPE/UFRJ, Rio de Janeiro, Brazil (in Portuguese)

Anderson, O. B. and Douglas, A. G. (1970), Bonding, Effective Stresses and Strength of Soils, *J. Soil Mech. Found. Div., Proc. Am. Soc. Civ. Eng.* 96:1073-1077

Bea, R. G. 1960, An experimental study of cohesion and friction during creep in saturated clay. Master’s thesis to the University of Florida, 107 pp.

Bishop, A. W., and Henkel, D. J., 1962. *The Measurement of Soil Properties in the Triaxial Test*: London (Edward Arnold).

Bishop, A.W. & Lovenbury, H.T. 1969, Creep characteristics of two undisturbed clays, *Proc. 7th ICSMFE, Mexico, Vol. I, pp. 29-37.*

Bjerrum, L. 1973, “Problems of soil mechanics and construction on soft clays.”, *State-of-the-art-Paper to Session IV, 8th ICSM & FE, Moscow, Vol. 3, pp. 124, 134.*

Buisman, A. S. Keverling (1936), "Results of Long Duration Settlement Tests," *Proc., Intern. Conf. on Soil Mech. and Found. Engr., Vol. 1, pp. 103-106.*

Casagrande, A. and Wilson, S.D. (1951) Effect of rate of loading on strength of clays and shales at constant water content. *Geotechnique*, 2(3), 251-263.

Crawford, C.B. 1964. Interpretation of the consolidation test. *Journal of the Soil Mechanics and Foundation Division, ASCE*, 90:

Finn, W. D., and Snead, D. E., (1973), “Creep and creep rupture of an undisturbed sensitive clay”, *Proc. 8th International Conference on Soil Mechanics and Foundation Engineering. Moscow, USSR.*

Glasstone, S., Laidler, K. J., & Eyring, H., 1940, *Theory of Rate Processes*. First Edition, New York: McGraw-Hill Book Co.

Kutter, B.L., and Sathialingam, N., (1992), Elastic–viscoplastic modelling of the rate-dependent

behaviour of clays. *Géotechnique*, 42(3): 427–441.

Lacerda, W.A., 1976, Stress Relaxation and Creep Effects on Soil Deformation, Ph.D. Thesis, University of California, Berkeley.

Leroueil, S., Kabbaj, M., Tavenas, F., and Bouchard, R., (1985), Stress-strain-strain rate relation for the compressibility of sensitive natural clays.” *Geotechnique*, 35(2), 159-180.

Lo, K. Y., (1969a), The pore pressure – strain relationship for normally consolidated undisturbed clays, Part I Theoretical considerations. *Canadian Geotechnical Journal* 6(4): 383-394.

Lo, K. Y., (1969b), The pore pressure – strain relationship for normally consolidated undisturbed clays, Part II Experimental Investigation and practical application. *Canadian Geotechnical Journal* 6(4): 395-412.

Martins, I. S. M., (1992), Fundamentals of a Behavioral Model for Saturated Clayey Soils, D.Sc. thesis, COPPE/UFRJ, Rio de Janeiro, Brazil (in Portuguese)

Mesri, G., Febres-Cordero, Shields, E., D. R., and Castro A., (1981), Shear Stress- Strain--Time Behavior of Clays, *Géotechnique*, 31, 4 pp. 537–552.

Mitchell, J. K., 1964, Shearing resistance of soils as a rate process. *Journal of the Soil Mechanics and Foundations Division, ASCE*, 90(1): 29–61.

Mitchell, J. K., Campanella, R. G., and Singh, Awtar, (1968) Soil creep as a rate process: *J. Soil Mech. Found. Div. Am. Soc. Civil Engrs* 94, No. SM1, Proc. Paper 5751,231-253.

Murayama, S. and Shibata, T., (1958), On the rheological characters of clay. Disaster Prevention Research Institute, Kyoto University, Bulletins, Bulletin No. 26, pp. 1-43.

Murayama, S. & Shibata, T. (1961), Rheological properties of clays, Proc. 5th ICSMFE, Vol. I, pp. 269-273.

Murayama, S., and Shibata, T., (1964) Flow and stress relaxation of clays Proceedings of I UTAM T Symposium on Rheology and Soil Mechanics, Grenoble Springer Verlag pp. 99-129.

Schmertmann, J.H. and Hall, J.R. Jr., (1961), “Cohesion after Non-Hydrostatic Consolidation”, ASCE, *Journal of the Soil Mechanics and Foundations Division*, Paper 2881, pp. 39-60.

Sekiguchi, H., (1984), Theory of undrained creep rupture of normally consolidated clay based on elasto- viscoplasticity, *Soils and Foundations* Vol. 24, No. 1, pp. 129- 147, Japanese Society of Soil Mechanics and Foundation Engineering.

Sherif, M.A. (1965), “Flow and Fracture Properties of Seattle Clays”, Research series No. 1, University of Washington Soil Engineering, January 1965.

Tavenas, F., Leroueil, S., LaRochelle, P. and Roy, M. (1978). “Creep behaviour of an undisturbed lightly overconsolidated clay”. *Canadian Geotechnical Journal*, Vol 15, pp.402-423.

Taylor, D. W., (1942), Research on Consolidation of Clays, publication From Department of Civil & Sanitary Engineering, MIT, Publication (Serial 82)

Taylor, D. W., (1948), *Fundamentals of Soil Mechanics*, John Wiley & Sons, New York.

Terzaghi, K., (1941), *Undisturbed Clay Samples and Undisturbed Clays*, *Journal of the Boston Society of Civil Engineers*, Vol. 28, No. 3, pp. 211-231.

Vaid (2004), Personal communication.

Vaid, Y. P. & Campanella, R. G. (1977), *Time-dependent behaviour of undisturbed clay*, *ASCEJ. Geotech. Engng* 103, No. 7, 693–709.

Vialov, S. S. and Skibitsky, A. M. (1957) *Rheological Processes in Frozen Soils and Dense Clays*, *Proc. 4th. International Conference on Soil Mechanics and Foundation Engineering*, p. 125.